

PURIFICATION AND BIOCHEMICAL CHARACTERIZATION OF FEN1: A
STRUCTURE SPECIFIC ENDONUCLEASE FROM *Xiphophorus maculatus*

THESIS

Presented to the Graduate Council
of Texas State University-San Marcos
in Partial Fulfillment
of the Requirements

for the Degree

Master of SCIENCE

by

Arnold P. Ruymgaart, B.S.

San Marcos, Texas
May 2005

COPYRIGHT

by

Arnold Peter Ruymgaart

2005

ACKNOWLEDGEMENTS

I would like to thank Dr. Ronald Walter for accepting me into his research group and providing me with a position in his laboratory for the duration of my time as graduate student at Texas State University-San Marcos. In addition, he has provided me with much guidance and encouragement.

I would also like to thank Dr. Kevin Lewis and Dr. Rachell Booth for always taking the time to answer my questions and for their guidance.

My parents, Frits and Marsha Ruymgaart, have also provided tremendous support and their interest in my work has been a continuous source of motivation.

Finally, I would like to thank Sheila Heater, Leon Oehlers, and Melissa Wells for their patience, extensive help, and willingness to offer their own time to help me advance.

This manuscript was submitted to the committee on March 11, 2005.

TABLE OF CONTENTS

ACKNOWLEDGEMENTS	iv
LIST OF TABLES	vi
LIST OF FIGURES	vii
ABSTRACT	ix
CHAPTER	
I. INTRODUCTION	1
II. MATERIALS AND METHODS	9
III. RESULTS	23
IV. DISCUSSION	57
LITERATURE CITED	65

LIST OF TABLES

<u>Table #</u>	<u>Page #</u>
2-1 Oligonucleotides used in cloning and overexpression studies of xiFEN1	12
3-1 Comparison of xiFEN1 amino acid sequence with sequences of other vertebrates	25
3-2 MALDI-TOF MS analyses of xiFEN1 tryptic peptides	41
3-3 Variance in specific activity with change in substrate and cofactor	49
3-4 Michaelis-Menten kinetic data derived from experiments using single flap substrate and manganese or magnesium cofactor	52

LIST OF FIGURES

<u>Figure #</u>	<u>Page #</u>
1-1 Expected FEN1 substrates <i>in vivo</i>	3
1-2 The "Gordon-Kosswig" melanoma model interspecies backcross	7
2-1 Substrates used in the xiFEN1 characterization studies	19
3-1 Comparison of deduced amino acid sequences for <i>Xiphophorus</i> , zebrafish, frog, mouse and human FEN1	26
3-2 Structure of the xiFEN1 gene	28
3-3 Cloning of the xiFEN1 open reading frame for recombinant expression in <i>E. coli</i>	33
3-4 Recombinant expression of xiFEN1 in <i>E. coli</i>	35
3-5 Purification of recombinant xiFEN1	37

3-6 MALDI-TOF MS analysis of xiFEN1ct	39
3-7 Activity and substrate specificity of xiFEN1 and hFEN1	43
3-8 Determination of steady state kinetic parameters for xiFEN1 and hFEN1 using single flap substrate	50
3-9 Influence of temperature on xiFEN1 and hFEN1 enzymatic activity	53
3-10 XiFEN1 and hFEN1 cleavage site preference at varying temperature and cofactors	55

ABSTRACT

PURIFICATION AND BIOCHEMICAL CHARACTERIZATION OF FEN1: A
STRUCTURE SPECIFIC ENDONUCLEASE FROM *Xiphophorus maculatus*

by

Arnold Peter Ruymgaart, B.S.

Texas State University-San Marcos

May 2005

SUPERVISING PROFESSOR: RONALD WALTER

Flap endonuclease-1 (FEN1) is a structure specific 5' endo/exonuclease involved in DNA replication and repair. Presented herein are the cloning, gene structure, recombinant expression and characterization of flap endonuclease-1 (xiFEN1) from *Xiphophorus maculatus*. The xiFEN1 gene structure was found to include 8 exons and 7 introns. The *Xiphophorus* FEN1 cDNA sequence harbored an open reading frame that encodes a 380 amino acid protein with a predicted mass of 43 kDa. The intact FEN1 cDNA was subcloned into a set of

bacterial expression vectors (pET101-xiFEN1ct, pET100-xiFEN1nt and pET101-xiFEN1wt) and recombinant xiFEN1 enzyme purified from *E. coli* cell extracts. The pET-xiFEN1 fusion translation products were tagged with a ~3 kDa vector-encoded carboxy (pET101-xiFEN1ct) or amino (pET100-xiFEN1nt) terminal extension designed to facilitate protein recognition and purification. The xiFEN1 fusion proteins were purified and their amino acid sequences verified by Western blotting and tryptic peptide mass fingerprinting. The purified recombinant proteins were assessed for enzyme activity and specificity using several different oligonucleotide substrates. Results presented establish differences in kinetic parameters, substrate and product preference, and response to changes in temperature and metal ion cofactor for xiFEN1 activity compared to the human FEN1 protein.

CHAPTER I

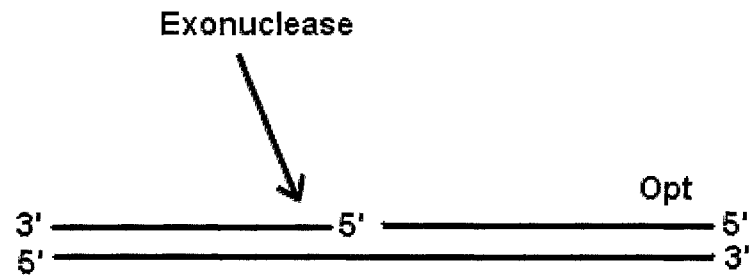
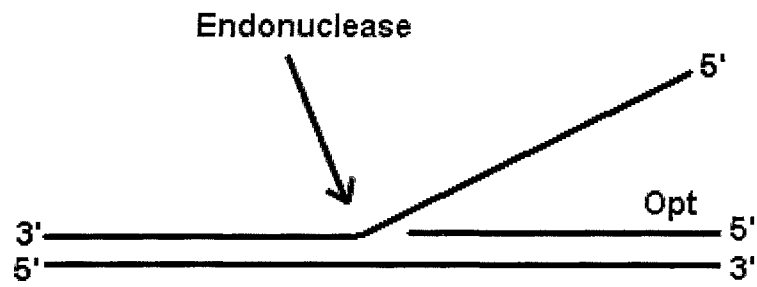
INTRODUCTION

The human flap endonuclease-1 gene (hFEN1) encodes a soluble 43 kDa enzyme important for DNA repair and replication. FEN1 endonuclease activity removes 5' flap structures that may be created by strand displacement during DNA repair or replication (Figure 1-1). Additionally, FEN1 is involved in processing of Okazaki fragments during completion of lagging strand synthesis (1). In DNA repair FEN1 has been shown to be involved in both nucleotide excision repair (NER) and base excision repair (BER) pathways (2, 3). In cultured cells and yeast, FEN1 gene knockout studies have shown pleiotropic deficiencies in DNA metabolism hallmarked by decreased resistance to DNA alkylating agents, increased spontaneous mutation incidence, microsatellite instability, and a shortened cellular lifespan (4, 5). FEN1 has also been shown to be involved in disorders correlated with DNA repeat expansion in higher organisms (6, 7).

Important FEN1 structural features include two functional domains involved in DNA binding and catalysis, a flexible loop that is thought to wrap single-strand (flap) DNA, and a region near the carboxy terminus involved in PCNA binding (3, 8, 9, 10). The FEN1 active site employs two divalent cation

cofactors which are coordinated by 7 highly conserved acidic residues; D34, D86, E158, E160, D179, D181 and D233 (8, 10). These metal ion cofactors are required for substrate binding and catalysis (8, 10, 11, 12). FEN1 has been studied within widely divergent experimental systems represented by bacteria, yeast, and mammalian cells (i.e., both rodent and human forms). Results from these studies show discrete differences (such changes in enzyme activity with changes in temperature, pH and concentration of various metal ions; 9, 13, 14) in prokaryotic, yeast and mammalian forms of FEN1 and suggest data in fishes, as stem vertebrates, may provide an interesting point of comparison (13, 14).

Figure 1-1: Expected FEN1 substrates *in vivo*. Simplified diagram of DNA structures that may be expected FEN1 endo- and exonuclease substrates *in vivo*. The endonuclease substrate features a 5' single stranded overhang ("flap") and may be formed by displacement synthesis in a gap filling step during DNA repair or replication. Potential FEN1 exonuclease substrates (gapped, nicked or 5' recessed structures) could be generated in various pathways of DNA metabolism. Other substrates with known FEN1 activity can be created from these basic structures by removing or modifying the optional (Opt) adjacent strand.



The genus *Xiphophorus* is an important vertebrate model for investigating the etiology and genetics of both spontaneous and induced cancers (for review see 15). *Xiphophorus* are comprised of 26 species most of which can be crossed to produce fertile interspecies hybrid progeny. The *Xiphophorus* gene map is well developed (16, 17) and allows genetic associations to be studied among cohorts of progeny derived from backcrossing interspecies hybrid animals to one of the parental strains (16, 17). Ionizing radiation, ultraviolet light (UVB) exposure, and exposure to methylnitrosourea (MNU) have all been shown to induce diverse types of tumors (i.e., melanoma, renal carcinoma, neurofibrosarcoma, schwannoma, retinoblastoma) within cohorts of specific *Xiphophorus* interspecies hybrid backcrosses (18, 19, 20, 21). These inducible tumor models are dependent upon; simply backcrossing an F₁ interspecies hybrid to the parental line to produce first backcross generation (BC₁) animals (i.e. "spontaneous" tumorigenesis); or models that require exposure of BC₁ hybrids to DNA damaging agents to induce the tumor phenotype (i.e. inducible tumorigenesis; Figure 1-2).

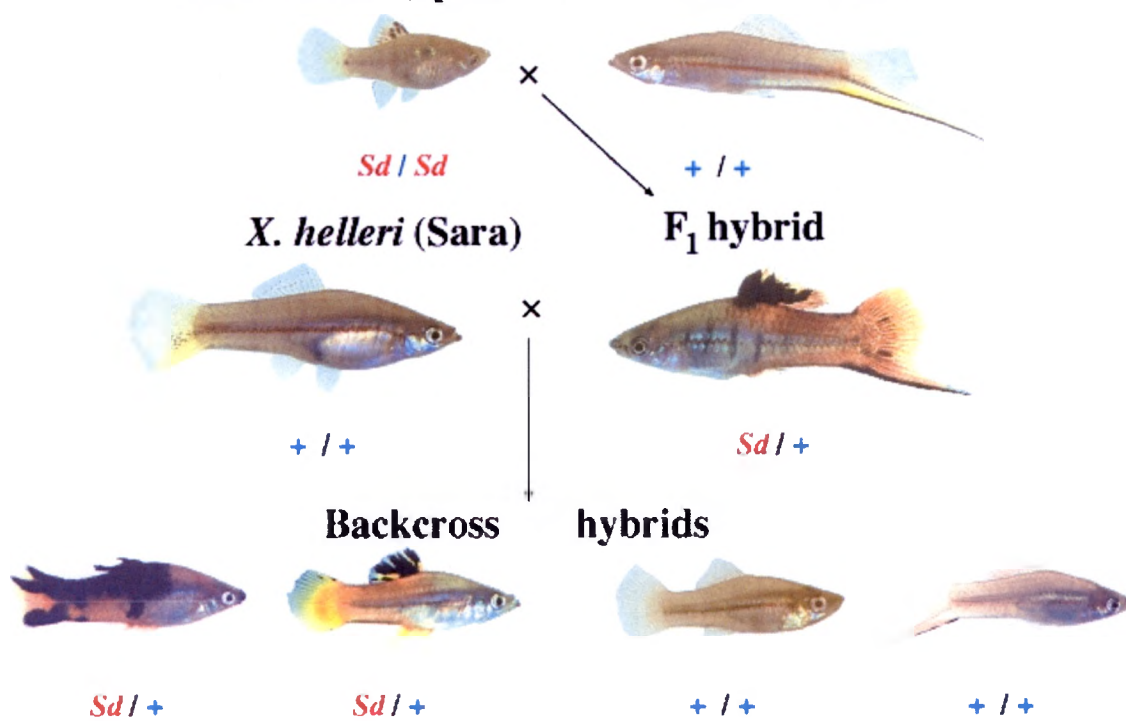
For inducible tumor models, the requirement of exposure of BC₁ fish to DNA damaging agents and well-established hybrid genetics make the *Xiphophorus* experimental system an excellent model to study the contribution of DNA repair capability to tumor predisposition. Accordingly, major DNA repair pathways, including NER and BER have been shown to exhibit modulated repair capability within select tissues of interspecies hybrid animals when compared to the repair capacities in the same tissues of parental species (22, 23, 24, 25).

These results indicate there may be reduced DNA repair function in select hybrid fish tissues and thus it is of interest to determine if predisposition to induced tumor development is correlated with specific loss or gain of DNA repair capability that may be brought about solely by the mixing of alleles that occurs upon interspecies hybridization. Study of DNA repair pathways in hybrids may lead to a greater understanding of repair in general and allelic interplay within multigenic traits in particular. DNA repair has been studied primarily in bacteria, yeast, and mammalian cells. There exists a paucity of information regarding DNA repair gene regulation and DNA repair protein biochemistry within fishes as a point of comparison with mammalian forms. To approach these types of questions and to provide comparative DNA repair data we have initiated the systematic characterization of DNA repair genes and proteins involved in the BER pathway. Herein we report the cloning, gene structure, recombinant expression and primary enzymatic activities of the *X. maculatus* Jp 163 A DNA repair gene encoding flap endonuclease-1 (xiFEN1).

Figure 1-2: The "Gordon-Kosswig" interspecies melanoma model. Loci derived from the *Xiphophorus maculatus* Jp 163 A strain, carrying the "spotted dorsal" trait (Sd) are colored red; and the corresponding loci from the swordtail (*Xiphophorus helleri*) are colored blue. When F₁ progeny are backcrossed to the *Xiphophorus helleri* parental line, 25% of BC₁ hybrids (bottom left) develop invasive melanoma resulting in necrosis of the dorsal fin region (spontaneous melanomagenesis).

The "Gordon-Kosswig" (H005BC₁-B) Cross

X. maculatus (Jp 163 A) *X. helleri* (Sara)



CHAPTER II

MATERIALS AND METHODS

Animals, tissue dissection and nucleic acid isolation:

Mature male *Xiphophorus maculatus* (strains Jp 163 A and B) from highly inbred lines (>90 generations) were obtained from the *Xiphophorus* Genetic Stock Center, Texas State University, San Marcos, Texas (www.xiphophorus.org). Fish were euthanized in a solution of 3-aminobenzoic acid ethyl ester methanesulfonate (MS-222; Sigma, St. Louis, MO). Brain, eye, gill, liver, testis and skin tissues were dissected and individually flash frozen or submerged in "RNA later" (Ambion, Austin, TX) and stored at -80°C.

Genomic DNA was extracted with a Puregene DNA purification kit (Gentra, Minneapolis, MN) following the manufacturer's protocol. RNA from each tissue was extracted with TriReagent (Sigma) using the manufacturer's instructions, and treated with DNase I to remove co-extracted DNA. Quantities of DNA and RNA were determined via fluorimetry employing either the PicoGreen DNA or the RiboGreen RNA quantification kit (Invitrogen, Carlsbad, CA) using a BioTek FLx800 microplate fluorometer (BioTek, Winooski, VT).

cDNA synthesis and cloning of the *Xiphophorus FEN1* gene:

Complementary cDNA was synthesized from *Xiphophorus* RNA using a SuperScript™ First-Strand Synthesis kit (Invitrogen) following the manufacturer's instructions. cDNA synthesis was catalyzed using SuperScript™ II reverse transcriptase primed with oligo(dT).

Degenerate primers were designed based on vertebrate FEN1 sequences available in public databases for the primer-directed amplification of xiFEN1 from *Xiphophorus* testis cDNA. Areas of highly conserved sequence were observed from the alignment of medaka, frog, chicken and human DNA sequence. The degenerate primers were designed in these highly conserved regions. An initial 430 bp amplicon was produced via 2 rounds of nested-primer PCR amplification using Taq polymerase (Invitrogen) and primers shown in Table 2-1. The 430 bp amplicon was cloned into the pCR®2.1-TOPO vector (Invitrogen). Nucleotide sequences from mini-preparations of plasmid clones were determined using M13 forward and reverse primers (Davis Sequencing, LLC., Davis, CA).

To amplify and clone the 5'- and 3'- ends of xiFEN1 we utilized 5'- and 3'- RACE kits (Invitrogen) following the manufacturer's instructions using testis cDNA as a target. A nested-primer PCR strategy was employed using the primers listed in Table 2-1 to amplify a 558 bp sequence from the 5'- region and a 580 bp sequence from the 3'-region of the xiFEN1 cDNA. Each amplicon was subcloned and its nucleotide sequence determined as described above. All sequences were aligned using the MacVector™ software package (version 7.0)

and computer-spliced to create a single contiguous 1,356 bp sequence representing the complete xiFEN1 coding sequence.

Gene structure:

The *Xiphophorus* cDNA sequence obtained was used to allow design of gene-specific primers for sequential screening of *Xiphophorus* genomic DNA for the presence of intron regions. PCR amplification using various gene-specific primer pairs, cloning of amplimers, nucleotide sequencing, and sequence analyses were performed as described above.

Table 2-1: Oligonucleotides used in the xiFEN1 cloning and overexpression studies.

Identity	Oligonucleotide Sequence
Degenerate FEN1 Primers¹	
Fen1 F1	5'-CAYYTIATGGGNATGTTYTA-3'
Fen1 F2	5'-TAYGTITTYGAYGGNAARCC-3'
Fen1 R1	5'-CAIARRTCIACRAAYTGYTC-3'
Fen1 R2	5'-TCYTTRTGIARCCARTTYTC-3'
Coding Sequence Primers	
FEN1 CDSf	5'-ATGGGAATTCACGGACTGGC-3'
FEN1 CDSf2	5'-CACCATGGGAATTCACGGACTGGC-3'
FEN1 CDSr	5'-TCAGAGTTCAGTCTATTTGCCCTT-3'
FEN1 CDSr2	5'-TTTGCCCTTCCTAAATTTGCCTGG-3'
5'- and 3' – RACE primers	
Fen1 5'-RACE 2	5'-GCAGTGAGGTGTCTTAGCAGGA-3'
Fen1 5'-RACE 3	5'-CATAACGACGATTGCAAGAAGC-3'
Fen1 3'-RACE 1	5'-TGCTAAGACACCTCACTGCCAGT-3'
Fen1 3'-RACE 2	5'-TCGTATCCTGCAGGACATCGGT-3'
Substrate Oligonucleotides	
Sub-Br	5'-GGACTCTGCCTCAAGACGGTAGTCAACGTG-3'
Sub-Flap	5'-GATGTCAAGCAGTCCTAACTTTGAGGCAGAGTCC-3'
Sub-Adj1	5'-CACGTTGACTACCGTC-3'
Sub-Adj2	5'-CACGTTGACTACCGTCC-3'
Sub-Gpstr	5'-TGAGGCAGAGTCC-3'

¹Standard mixed base definitions are: Y = C,T; N = A,C,G,T; R = A,G.

Cloning of the xiFEN1 open reading frame:

To obtain an intact and complete coding sequence, a pair of forward and reverse primers (Table 2-1; FEN1 CDSf and FEN1 CDSr) were designed to initiate amplification at the start codon and at a site ending 12 nucleotides downstream from the *Xiphophorus* stop codon within the 3'-untranslated region (3-UTR). This primer pair was used to PCR amplify brain-derived cDNA. Upon amplification a single PCR product of expected size (~1100 bp) was observed by agarose gel electrophoresis (Figure 3-3A). The amplicon was extracted from the gel and subcloned into the pCR[®]2.1 vector (Invitrogen) without specific directional orientation. After transformation several plasmid subclones appeared to contain an insert upon restriction digest of extracted plasmid DNA (Figure 3-3B). These subclones were isolated and nucleotide sequences determined to identify a clone appropriate for recombinant bacterial expression and protein purification.

Expression and purification of xiFEN1:

A pair of primers was designed to promote directional cloning of the xiFEN1 coding sequence into the pET expression vector by PCR amplification of archived template. The forward primer (Table 2-1; FEN1-CDSf2) was modified from the one used to clone the coding region by addition of a 4-base upstream extension. This extension produced a sequence complementary to the vector at the 5' end of the amplification product. A new reverse primer (FEN1-CDSr2) was designed to end at the base immediately prior to the native stop codon, allowing

the latter to be removed for production of the xiFEN1ct insert. This insert was designed to be placed in the pET101 vector. The pET100 insert (xiFEN1nt) and the pET101 wild-type insert (xiFEN1wt) were identical and similar to the xiFEN1ct insert except the FEN1 CDSr primer was used, leaving the native stop codon in place. The combined pET vector strategy allowed the simultaneous production of a carboxy terminal fusion product (xiFEN1ct), an amino terminal fusion product (xiFEN1nt) and a wild-type product. A high fidelity polymerase (Pfx, Invitrogen) was utilized in these PCR reactions and all temperature programs consisted of a 5 min. denaturation at 94°C, 35 amplification cycles (94°C for 15 sec., 54°C for 30 sec., 68°C for 1 min.) and a final extension at 68°C for 7 min (Figure 3-3C).

The amplified coding regions were subcloned into the pET expression vector to produce plasmids pET101-xiFEN1ct, pET100-xiFEN1nt and pET101-xiFEN1wt. These constructs were transformed into chemically competent TOP10™ *E. coli* cells (Invitrogen) for archived storage. The resultant bacterial cultures were verified for propagation of plasmids with the correct insert and orientation by PCR analysis of extracted DNA, using vector-specific forward, and gene-specific reverse primers (Figure 3-3D). Plasmid DNA's from clonal *E. coli* cultures used for overexpression were confirmed by dideoxynucleotide sequencing (Davis Sequencing) to carry the correct reading frame and stored at -80°C in 50% glycerol.

The pET-xiFEN1 vector constructs were purified from archive culture and transformed into BL21Star(DE3) *E. coli* cells (Invitrogen). Cultures were grown

overnight at 37°C after which induction of expression was accomplished by addition of isopropyl-β-D-thiogalactoside (IPTG, 1 mM) to the cells.

Recombinant protein expression was induced by addition of IPTG (1 mM) to the culture media followed by incubation at 37°C with aeration. Culture samples were taken at each hour after induction (Figure 3-4A, B and C). Generally, large-scale preparations were grown in 500 mL of tryptone broth culture media (10 gm tryptone, 5 gm yeast extract, 5 gm NaCl per liter) to sufficient density followed by 4 to 6 hrs of incubation after addition of the inducer (IPTG). Cells were harvested by centrifugation (3,000 X g, 15 min.) and stored at -80°C after addition of 50% glycerol. Lysis was accomplished by resuspension of the cell pellet in 10 mL native purification buffer (50 mM sodium phosphate pH 8, 500 mM NaCl; 1 mg/mL lysozyme) followed by bath sonication (3 pulses, 15 sec.) and 3 rapid freeze-thaw cycles. The cell extract suspension was cleared by centrifugation (17,000 x g, 25 min.).

To purify the xiFEN1 fusion proteins the soluble extract fraction was loaded on an appropriately prepared and equilibrated Ni²⁺-nitrilotriacetate-agarose (Ni²⁺IMAC) column (Invitrogen). The column was then washed four times with wash buffer (50 mM sodium phosphate pH 8.0, 500 mM NaCl and 25 mM imidazole) to remove unbound proteins. Following washing, the bound proteins were eluted from the column by addition of elution buffer (purification buffer containing 250 mM imidazole). The eluate was collected in eight 1 mL fractions and aliquots of each fraction analyzed by sodium dodecyl sulfate polyacrylamide gel electrophoresis (SDS-PAGE). Fractions containing a protein

band of the expected size for xiFEN1 were dialyzed against FEN1 storage buffer (50 mM Tris-HCl pH 8.0, 50% (v/v) glycerol) for 12 hours at 4°C. Total protein amount was determined using the Bradford assay (BioRad Inc.). Purity was assessed via Coomassie stained SDS-PAGE gels (Figure 3-5A and 3-5B) and reached about 90%.

Analysis of xiFEN1 expression by SDS-PAGE and Western blot

Both crude cell lysate and Ni²⁺IMAC purification samples were analyzed using pre-cast Novex discontinuous 4-12% Bis-Tris polyacrylamide gels (Invitrogen; Figure 3-4A, 3-4B, 3-4C, 3-5A, 3-5B and 3-5C). Proteins were visualized with Coomassie stain (Pierce, Rockford, IL, USA) or transferred onto nitrocellulose membranes for Western blot analysis. Western blot membranes were probed with antibody immunoreactive to the fusion tag epitope (AntiV5™ or AntiXpress™ at a 1:5000 dilution, Invitrogen) or anti human FEN-1 (Trevigen, Gaithersburg, MD, USA). Detection of bound antibody was accomplished using chemiluminescence (WesternBreeze kit, Invitrogen) (Figure 3-4D and 3-4E).

All gel and Western blot images were captured and analyzed using a Kodak Digital Science Image Station 440CF employing Kodak 1D version 3.6.1 software (Eastman Kodak, New Haven, CT, USA).

Characterization of recombinant xiFEN1 by peptide mass fingerprinting:

Approximately 0.5 µg of gel-purified recombinant xiFEN1 was in-gel digested with trypsin. The resulting xiFEN1 peptides were extracted from the gel,

dried under vacuum, and resuspended in 10% acetonitrile (in water) containing 0.1% trifluoroacetic acid. These samples were diluted 1:5 in 20 mg/mL α -cyano-4-hydroxycinnamic acid (CHCA) matrix solution, and 0.5 μ L was spotted onto a MALDI target plate. Spectra were acquired with a Bruker Autoflex TOF/TOF mass spectrometer (Bruker Daltonics, Billerica, MA) in externally calibrated reflectron mode and represent the average of 400 laser shots from a 337-nm nitrogen laser (26).

Preparation of Substrates:

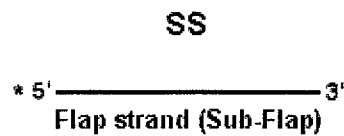
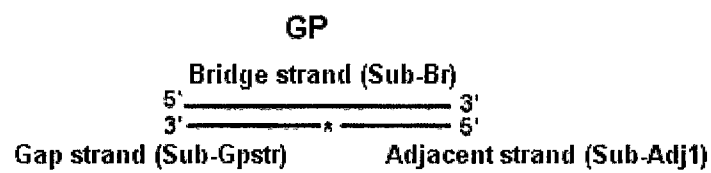
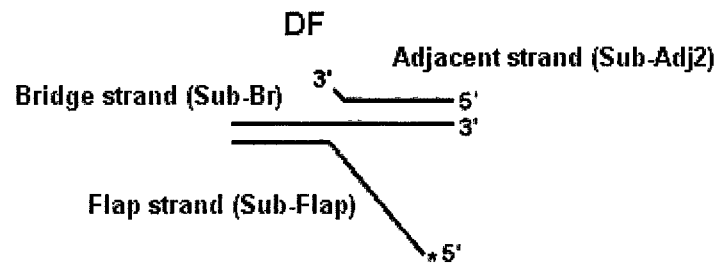
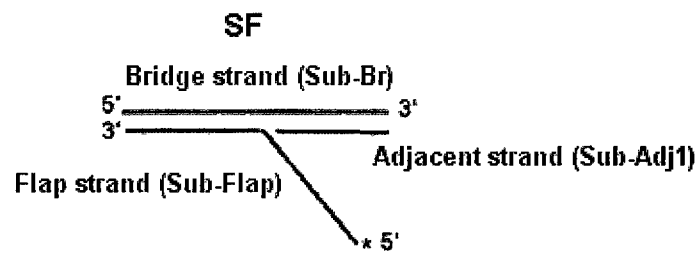
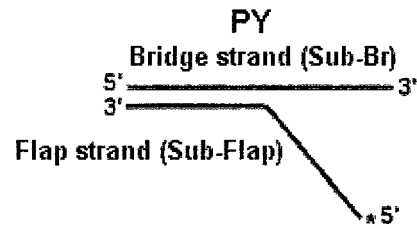
Five oligonucleotide substrates were prepared to assess xiFEN1 enzymatic activity (see Figure 2-1). Oligonucleotides were PAGE purified and identical in sequence to those previously described (3, 13) for substrates PY and SF. The flap strand (Table 2-1, Sub-Flap) or gap strand (Table 2-1, Sub-Gpstr) oligonucleotide was 5' radiolabeled in a T4 polynucleotide kinase catalyzed reaction utilizing 1.7 μ M γ^{32} P ATP (Perkin Elmer). Radiolabeling reactions were performed at 37°C for 30 min. followed by 75°C for 5 min. to terminate the reaction. Radiolabeled samples were desalted by size exclusion chromatography (SEC) utilizing a Microspin™G25 column, (Amersham, Piscataway, NJ, USA) centrifuged at 750 x g for 2 min.

To create substrates SF, DF and GP, the radiolabeled flap or gap strand was annealed to a two-fold excess of both the bridge (Table 2-1, Sub-Br) and adjacent strands (Table 2-1, Sub-Adj1 for substrates SF and GP or Sub-Adj2 for substrate DF) in annealing buffer (20 mM Tris-HCl pH 7.4, 150 mM NaCl).

Substrate PY was annealed as above except in presence of the bridge strand only. The annealing temperature profile included 5 min. incubation at each of the following temperatures using an Applied Biosystems 2700 thermocycler; 99°C, 80°C, 70°C, 60°C, 58°C, 56°C, 54°C, 52°C, 50°C, 45°C, 35°C and 25°C.

Figure 2-1: Substrates used in the xiFEN1 characterization studies. These substrates were prepared by annealing the appropriate oligonucleotides as described (see Table 2-1).

* Indicates radio label



All substrates were dried in a vacuum centrifuge and stored at -20°C for no more than three days prior to use. Quantification of substrate final products consistently demonstrated ~60% recovery, estimated using initial amounts of oligonucleotides and taking into account the stoichiometry of the annealing reaction.

Activity, substrate specificity, kinetic and temperature assays:

Assays were performed as described by Harrington and Lieber (1994) with the following modifications. Reactions were run in a PCR machine and mixture components were added in the following order: sterilized water, reaction buffer (50 mM Tris-HCl pH 8.0, 10 mM MnCl₂ or MgCl₂, 1 mM DTT and 0.1 mg/mL BSA), labeled substrate, and finally a catalytic amount of the enzyme (when the reaction tube reached 4°C). All reactions were carried out in 20 µl volumes at the following temperature profile: an initial hold at 4°C for 2 min. during which the enzyme was added, a reaction period of 10 min. at 30°C, and finally a hold at 4°C for 2 min. during which stop/dye solution (bringing the final mixture to 50 mM EDTA) was added. Samples were denatured at 85°C for 5 min. before loading on 20% denaturing (7M urea) PAGE gels (43 cm) in 1X TBE and were run at 1700 V for 3 hours to fractionate FEN1 reaction products.

Kinetic assays were performed identically except that initial substrate concentration was varied (Figure 3-8). Similarly, in temperature assays, only the temperature maintained during the reaction period was varied from the above mentioned procedure (Figure 3-9).

Prior to electrophoresis the radioactive content of all labeled products and stock substrates was determined using a Beckman LS6000IC (Beckman, Fullerton CA) scintillation counter to determine labeling efficiency and calculate specific activities. Initial substrate concentrations were obtained from these data for each sample and usually differed by less than 10% from the expected amount delivered.

After electrophoresis the gels were used to expose super-resolution phosphor imager screens (Packard, Meriden, CT) and final substrate-product fractions obtained by comparing gross digital light unit (DLU) intensities of areas encompassing each respective gel band in an experimental lane. The DLU data were obtained using a Packard Cyclone™ phosphorimager (Packard, Meriden, CT) and accompanying software.

CHAPTER III

RESULTS

Structure of the *Xiphophorus FEN1* gene:

Complementary DNA synthesized from total RNA isolated from *Xiphophorus* testes tissue was screened with degenerate primers designed using vertebrate FEN1 sequences available in the public databases. Initial amplification of testes cDNA resulted in a 430-bp product having a nucleotide sequence that when translated produced an amino acid sequence homologous to human FEN1 between residues 83 (tyrosine) and 226 (leucine, Figure 3-1). This putative xiFEN1 cDNA nucleotide sequence was used to design gene-specific primers for 5'- and 3'-RACE reactions in order to clone the entire xiFEN1 coding region. The 5'-RACE reaction produced a fragment containing the xiFEN1 start codon and an additional 53 nucleotides upstream in the 5'-untranslated region. The 3'-RACE reaction resulted in a cloned fragment containing the stop codon plus 148 nucleotides of the 3' untranslated region. Nucleotide sequences derived from cloning the interior, 5', and 3' fragments were used to construct a 1,356-bp xiFEN1 cDNA harboring an 1,140-bp open reading frame (ORF) that, when translated, exhibited very high homology to other known FEN1 sequences. The 380 amino acid xiFEN1 protein is predicted to have a

mass of 42.7 kDa and is presented in Figure 3-1 aligned with zebrafish and human FEN1 sequences. Table 3-1 presents xiFEN1 identity and similarity values compared to FEN1 proteins from four species. XiFEN1 exhibits high identity (74% to 88%) and similarity (88% to 95%) to these other vertebrate FEN1 proteins.

A complete gene structure for a eukaryotic FEN1 gene had not been reported. Based on the xiFEN1 cDNA sequence, we designed primers spaced along the cDNA length and used these primers in PCR reactions using *X. maculatus* Jp 163 A genomic DNA as a target. Several of these reactions produced amplicons of varying lengths and all isolated fragments were subjected to nucleotide sequencing to identify intron regions. The complete gene structure of *Xiphophorus* FEN1 was determined and is shown in Figure 3-2A. The xiFEN1 gene spans 2.6 kb of genomic DNA and contains 7 introns ranging in size from 335- to 96-bp and 8 exons ranging in size from 400- to 40-bp (Figure 3-2B).

Table 3-1: Percent identity and similarity of FEN1 amino acid sequences for different vertebrates. Percent similarities are shown in parentheses. Similarities are based on amino acid functional groups where A=G=P=S=T, K=H=R, F=W=Y, I=L=M=V, D=E and N=Q; (30).

	<i>Xiphophorus</i>	Zebrafish	Frog	Mouse	Human
<i>Xiphophorus</i>	100 (100)	88 (95)	77 (89)	74 (87)	74 (87)
Zebrafish		100 (100)	79 (88)	76 (88)	76 (88)
Frog			100 (100)	81 (92)	80 (93)
Mouse				100 (100)	97 (98)
Human					100 (100)

Figure 3-1: Comparison of deduced amino acid sequences for *Xiphophorus*, zebrafish, frog, mouse and human flap endonuclease-1 (FEN1). Similar amino acids are marked with a "." and are blocked in teal. Identical amino acids are shown blocked in gray. Acidic residues involved in metal coordination (8, 10) are blocked in yellow. Basic residues involved in DNA binding are blocked in green (27). Changes of particular interest near conserved residues are blocked in red.

Xiphophorus 1 MGIHGLAKLIADHAPGAI~~NE~~EQIKNYFGRK~~IA~~IDASMC~~IYQFLI~~AV~~EQD~~G 50
Zebrafish 1 MGIHGLAKLIADHAPSAI~~NE~~HEIKSYFGRK~~IA~~IDASMC~~IYQFLI~~AV~~EQD~~G 50
Frog 1 MGIHGLAKLIADVAPAAI~~NE~~HDIKSYFGRK~~IA~~IDASMC~~IYQFLI~~AV~~EQD~~G 50
Mouse 1 MGIHGLAKLIADVAPSAI~~NE~~NDIKSYFGRK~~IA~~IDASMC~~IYQFLI~~AV~~EQD~~G 50
Human 1 MGIQGLAKLIADVAPSAI~~NE~~NDIKSYFGRK~~IA~~IDASMS~~IYQFLI~~AV~~EQD~~G 50
.

Xiphophorus 51 NVLQSE~~EG~~ETTSHLMGMFY~~ET~~IRM~~ENG~~IKPVYVFDGKPPQLKSAE~~LE~~KR 100
Zebrafish 51 NVLQNE~~EG~~ETTSHLMGMFY~~ET~~IRM~~ES~~GIKPVYVFDGKPPQLKSGE~~LE~~KR 100
Frog 51 NTLQNE~~EG~~ETTSHLMGMFY~~ET~~IRM~~EH~~GIKPVYVFDGKPPQMKSGE~~LA~~KR 100
Mouse 51 DVLQNE~~EG~~ETTSHLMGMFY~~ET~~IRM~~EN~~GIKPVYVFDGKPPQLKSGE~~LA~~KR 100
Human 51 DVLQNE~~EG~~ETTSHLMGMFY~~ET~~IRM~~EN~~GIKPVYVFDGKPPQLKSGE~~LA~~KR 100
.

Xiphophorus 101 GERRAEAEKMLAKAQELGEQENIDKFSKRLVKVTKQHND~~IE~~CK~~LL~~LMG~~I~~ 150
Zebrafish 101 VERRAEAEKLLAQAEAGEQENIDKFSKRLVKVTKQHNEE~~CK~~LLSLMG~~I~~ 150
Frog 101 SERRAEAEKLLAEAAEEAGEVENIEKFTKRLVKVTKQHNEE~~CK~~LLTLMG~~I~~ 150
Mouse 101 SERRAEAEKQLQQAQAEAGMEEVEKFTKRLVKVTKQHND~~IE~~CK~~HLL~~SLMG~~I~~ 150
Human 101 SERRAEAEKQLQQAQAAGAEQVEKFTKRLVKVTKQHND~~IE~~CK~~HLL~~SLMG~~I~~ 150
.

Xiphophorus 151 PYI~~AP~~CEAEASCAALVKEGKV~~FAT~~ATEDMDGLTFG~~IN~~VLRH~~L~~TASEAK 200
Zebrafish 151 PYI~~AP~~CEAEASCAALVKAGKV~~YAT~~ATEDMDGLTFG~~IT~~VLRH~~L~~TASEAK 200
Frog 151 PYV~~D~~APCEAEATCAALVKAGKV~~YAA~~ATEDMDALTFG~~IP~~VLRH~~L~~TASEAK 200
Mouse 151 PYL~~D~~AP~~SE~~AEASCAALAKAGKV~~YAA~~ATEDMDCLTFG~~IP~~VLRH~~L~~TASEAK 200
Human 151 PYL~~D~~AP~~SE~~AEASCAALVKAGKV~~YAA~~ATEDMDCLTFG~~IP~~VLRH~~L~~TASEAK 200
.

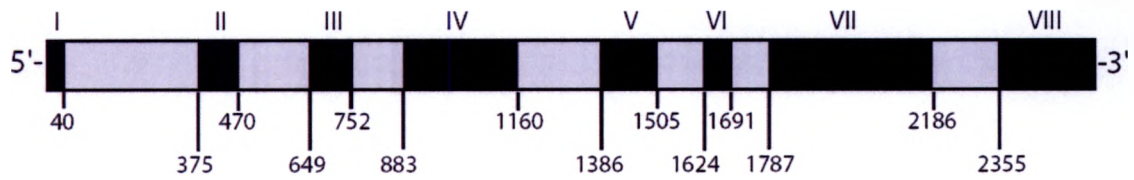
Xiphophorus 201 KLPIQEFHFNRILQDIGITSEQFIDLCILLGCDYCG~~II~~MGIGPKRAIDLI 250
Zebrafish 201 KLPIQEFHFSRILQDMELTHQQFIDLCILLGCDYCG~~II~~MGIGPKRAIDLI 250
Frog 201 KLPIQEFHLNRVIQDIGITHEQFIDLCILLGSDYCE~~II~~MGIGPKRAIDLI 250
Mouse 201 KLPIQEFHLSRVLQELGLNQEQFIDLCILLGSDYCE~~SI~~MGIGPKRAIDLI 250
Human 201 KLPIQEFHLSRILQELGLNQEQFIDLCILLGSDYCE~~II~~MGIGPKRAIDLI 250
.

Xiphophorus 251 RQHGSIEE~~IGEN~~IDTSKHPAPEDWLYKEARNLFLKPEV~~IDS~~STV~~L~~LKWRE 300
Zebrafish 251 KQHGSIEE~~IGEN~~IDPNKHPAPEDWLYKEARGLFLEPEV~~ID~~GSV~~L~~LKWNE 300
Frog 251 RQHTIDEI~~IDN~~IDLKKYPVPENWLHKEAKHLFLEPEV~~ID~~TDI~~T~~LKWIE 300
Mouse 251 QKHKSIEEIVRRILDPSKYVPENWLHKEAQLFLEPEV~~ID~~PESV~~L~~LKWSE 300
Human 251 QKHKSIEEIVRRILDPNKYVPENWLHKEAHQLFLEPEV~~ID~~PESV~~L~~LKWSE 300
.

Xiphophorus 301 PDE~~AL~~IQFMCSEKQFSE~~IR~~IRNGCK~~IM~~KSRQGSTQGR~~LD~~SFFSVTGS~~I~~ 350
Zebrafish 301 PDEDGLIQFMC~~AE~~KQFSE~~IR~~IRNGCK~~IT~~KSRQGSTQGR~~LD~~TFFFTVTGS~~I~~ 350
Frog 301 PDEEGLVAFMC~~GE~~KQFSE~~IR~~IRNGAKK~~IA~~KNRQGSTQGR~~LD~~DDFFKVTGS~~I~~ 350
Mouse 301 PNEEELVKFMC~~GE~~KQFSE~~IR~~IRSGVKRLSKSRQGSTQGR~~LD~~DDFFKVTGS~~I~~ 350
Human 301 PNEEELIKFMC~~GE~~KQFSE~~IR~~IRSGVKRLSKSRQGSTQGR~~LD~~DDFFKVTGS~~I~~ 350
.

Xiphophorus 351 SS-KRKEPETKGS~~KKK~~QKTGATP-GKFRK~~GK~~ 380
Zebrafish 351 SS-KRKEPETKGS~~AKK~~KQKTSATP-GKFKK~~GK~~ 380
Frog 351 SS~~IK~~RKEAESKGS~~AKK~~KAKTGGTPAGKFKR~~GK~~ 382
Mouse 351 SS~~IK~~RKEPEPKGPA~~AKK~~KAKTGG--AGKFR~~R~~GK 380
Human 351 SSAKRKEPEPKGST~~KKK~~KAKTGA--AGKFKR~~GK~~ 380
.

Figure 3-2: Structure of the *Xiphophorus* flap endonuclease-1 (*xiFEN1*) gene. **(A)** Exons are represented by the black boxes with the positions of the exon/intron boundaries listed. **(B)** Exon and intron sizes in the *Xiphophorus* FEN1 gene.

A**B**

Exon	Length (bp)	Intron	Length (bp)
I	40	1	335
II	95	2	179
III	103	3	131
IV	277	4	208
V	137	5	119
VI	67	6	96
VII	399	7	169
VIII	238		

Overexpression and purification of recombinant xiFEN1:

The *Xiphophorus* FEN1 ORF was cloned as a single fragment from brain tissue RNA (Figure 3-3A and 3-3-B) to allow subsequent subcloning into the pET plasmid (Figure 3-3C and 3-3D) for high level bacterial expression (Invitrogen). The constructed pET101-xiFEN1ct clone contained the intact xiFEN1 cDNA without its stop codon to allow read-through translation of the pET-101 vector encoded carboxy-terminal tag. The pET100-xiFEN1nt and pET101-xiFEN1wt clones contained the intact xiFEN1 cDNA with its stop codon in place. The pET100 vector provided an N-terminal extension. Both N- and C-terminal tags resulted in the xiFEN1 protein harboring an antigenic epitope plus six sequential histidine residues to facilitate Ni²⁺IMAC purification of the expressed fusion protein. The fusion proteins (i.e., epitope and His-tag) were predicted to have a mass of ~47 kDa, about 3 kDa more than the expected mass of ~44 kDa for xiFEN1wt.

BL21DE3 (Invitrogen) *E. coli* host cells were transformed with pET-xiFEN1 and exposed to IPTG to induce high-level expression of the xiFEN1 protein. Figure 3-4A, 3-4B and 3-4C show SDS-PAGE gels containing fractionated crude cellular lysate from *E. coli* samples at 2 and 5 or 6 hours post-induction. An increase in several proteins was observed in response to the IPTG treatment, including an increase in a protein band at the expected size of 47 or 44 kDa. Monoclonal antibody specific for the vector encoded epitope-tag was used in Western blotting of the crude *E. coli* extracts and the IPTG-inducible 47 kDa proteins were confirmed as the vector encoded translation products that are likely

the xiFEN1 fusion proteins (Figure 3-4E). Figure 3-4D displays a polyclonal anti-human FEN1 (Trevigen) Western blot of crude lysate containing xiFEN1ct. The additional bands correspond in size to those observed in the Coomassie stain gels of the same lysate samples (Figure 3-4B). They are therefore likely to be proteolytic fragments of the overexpressed protein. Western blots show the relative fragment amounts increase with time when probed with anti-human FEN1 antibodies but not when probed with the anti fusion-tag antibodies. These fragments may therefore not include the fusion tag antigenic epitope.

Single Ni²⁺IMAC purifications of large-scale (i.e., 500 mL culture) preparations of pET101-xiFEN1ct and pET101-xiFEN1nt transformed and IPTG-induced *E. coli* resulted in xiFEN1 fusion protein yields averaging 400 µg at a purity of >90% (Figure 3-5A and 3-5B). Cleavage of the xiFEN1nt N-terminal extension was attempted since unlike the carboxy terminal tag, it contained an enterokinase recognition site designed for removal of the tag. Cleavage of the fusion tag renders a recombinant protein differing in amino acid sequence from its natively translated counterpart by only a few amino acid residues remaining at the N-terminus. Under standard conditions, no measurable enterokinase cleavage activity was observed while a control protein identically tagged and expressed, (Polymerase Beta; 26) co-digested under these same conditions, did cleave as expected (Figure 3-5C, lanes 4 & 5). Additional EK digestions were attempted under various partially denaturing conditions (Figure 3-5C, lanes 1 and 2) and electrophoretic analysis of these digestion attempts revealed a faint band of expected product size at the 1M urea concentration (Figure 3-5C, lane 1).

Further increase in urea concentration appeared to induce non-specific EK cleavage activity but did not improve yield of desired product (Figure 3-5C, lane 2).

To confirm the correct proteins were isolated and to substantiate the correct translation of the xiFEN1 clones in the *E. coli* expression system, purified xiFEN1 fusion proteins were subjected to peptide mass fingerprinting (Figure 3-6). The mass fingerprints represent 53% coverage of the total xiFEN1ct amino acid sequence and 14% coverage of the total xiFEN1nt amino acid sequence (Table 3-2). These results confirmed the identity of the proteins purified as xiFEN1.

Figure 3-3: Cloning of the xiFEN1 open reading frame. All illustrations are digital images of 1% agarose gels stained with ethidium bromide under a UV light. **(A)** Results of PCR reactions designed to obtain the full length xiFEN1 coding region. Lane 2: positive PCR reaction control. Lanes 4 and 5: control reactions using the FEN1 CDSf and CDSr (Table 2-1) primers with opposing primers previously known to be functional. Resulting fragments were of the sizes expected. Lane 3: the amplicon produced with the CDSf and CDSr primer combination can be seen at about 1100 bp, the expected size of the xiFEN1 coding region. **(B)** Restriction digest (*EcoR* I, Invitrogen) of plasmid DNA extracted from cultures transformed with the pCR[®]2.1 vector containing the xiFEN1 coding region insert produced as illustrated in panel A. **(C)** Lane 2: PCR amplification of plasmid DNA harboring the xiFEN1 coding region insert using primer CDSf2 (Table 2-1) and high fidelity polymerase (Pfx, Invitrogen) to produce the inserts required for directional cloning into the pET expression vector. **(D)** PCR amplification of plasmid DNA extracted from cultures transformed with the pET100 vector containing the xiFEN1nt coding region insert produced as illustrated in panel C. Presence of the insert with correct directional orientation was verified by the use of vector specific forward and gene specific reverse primers. Positive results are observed only in lanes 4 and 8. Lane 10: positive PCR reaction control.

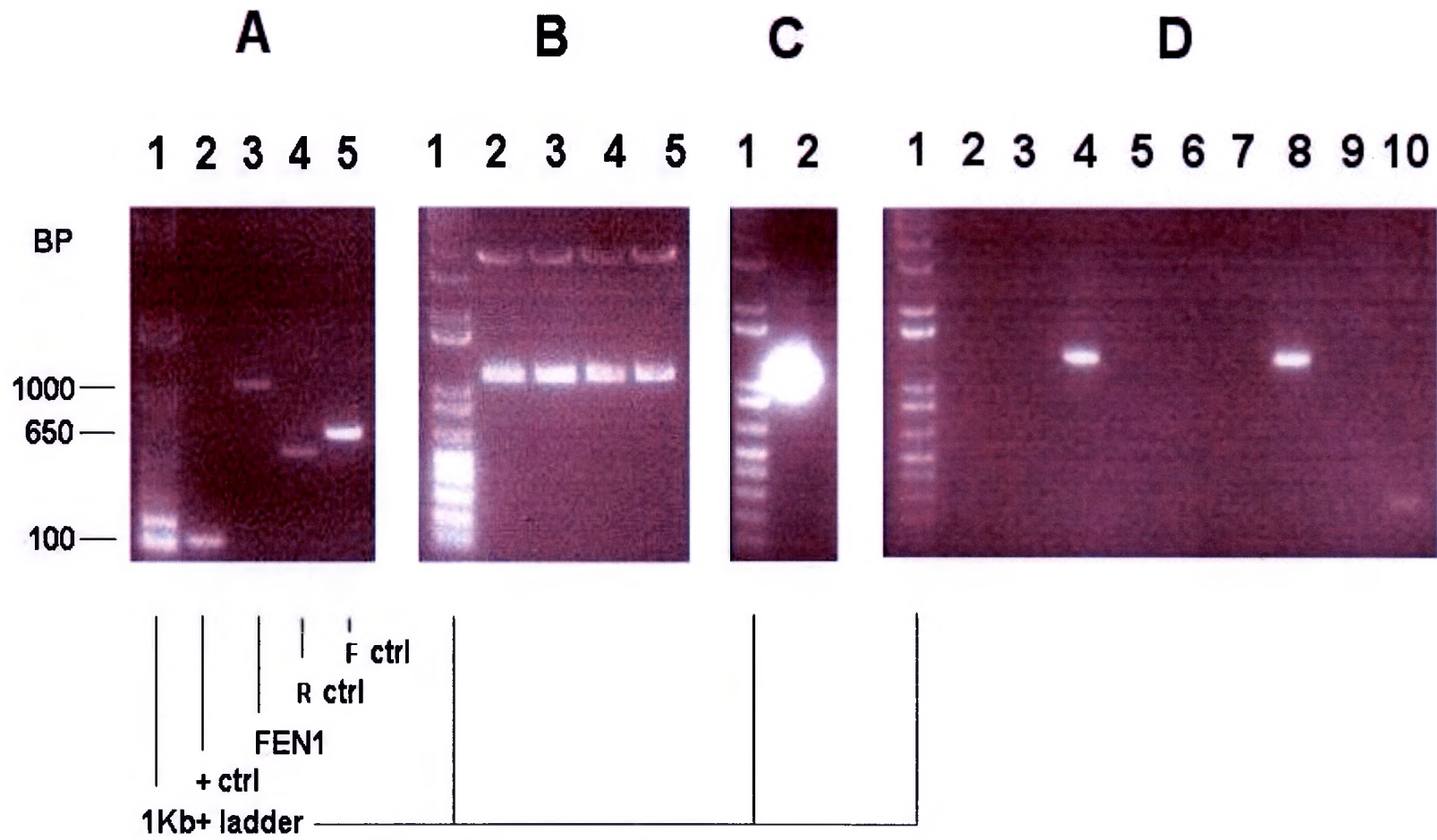


Figure 3-4: Expression of xiFEN1. **(A, B & C):** Analysis of crude cell lysate by SDS-PAGE, stained with Coomassie blue, of induced (+) or non-induced (-) cell culture fractions after the indicated time in hours of growth (above lane). In each case, a band of increasing intensity with induction time can be observed at the expected size of 44 or 47 kDa. **(D & E):** Chemiluminescence visualization of Western blot immunoreactivity utilizing polyclonal anti-human and monoclonal anti fusion tag specific antibodies respectively. The fractions of lysate samples used in this experiment were identical to those used to produce the results illustrated in panels A through C. Magic Mark™ (Invitrogen) was used as the molecular weight standard marker (stds) in both Western blots and Mark12™ (Invitrogen) in each Coomassie stained gel shown. Panel A: lysate samples containing xiFEN1wt. Panels B, D & E: lysate samples containing xiFEN1ct. Panel C: lysate samples containing xiFEN1nt.

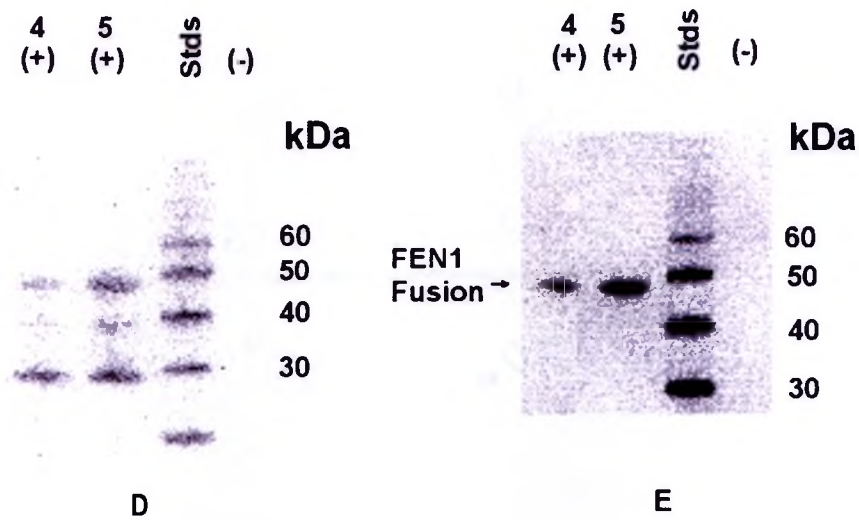
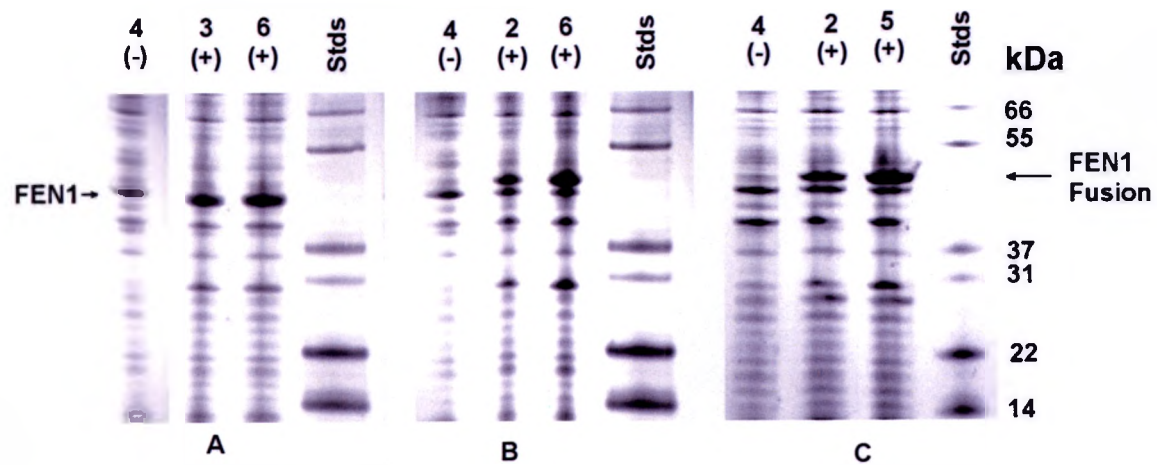


Figure 3-5: Purification of xiFEN1. **(A):** Analysis by SDS-PAGE (7-12% with Coomassie stain) of the xiFEN1ct single step IMAC purification product. **(B):** Analysis by SDS-PAGE of the xiFEN1nt single step IMAC purification product. **(C)** Enterokinase digest of xiFEN1nt (lanes 1 through 3) and control (lanes 4 & 5) under non- and partially-denaturing conditions: lane 1: 1M urea, lane 2: 2M urea and lanes 3, 4 and 5 no urea. No xiFEN1nt cleavage is observed without urea (lane 3). A faint band of expected size is observed at 1M urea. At 2M urea, it appears there may be non-specific cleavage and no additional product of correct size is observed.

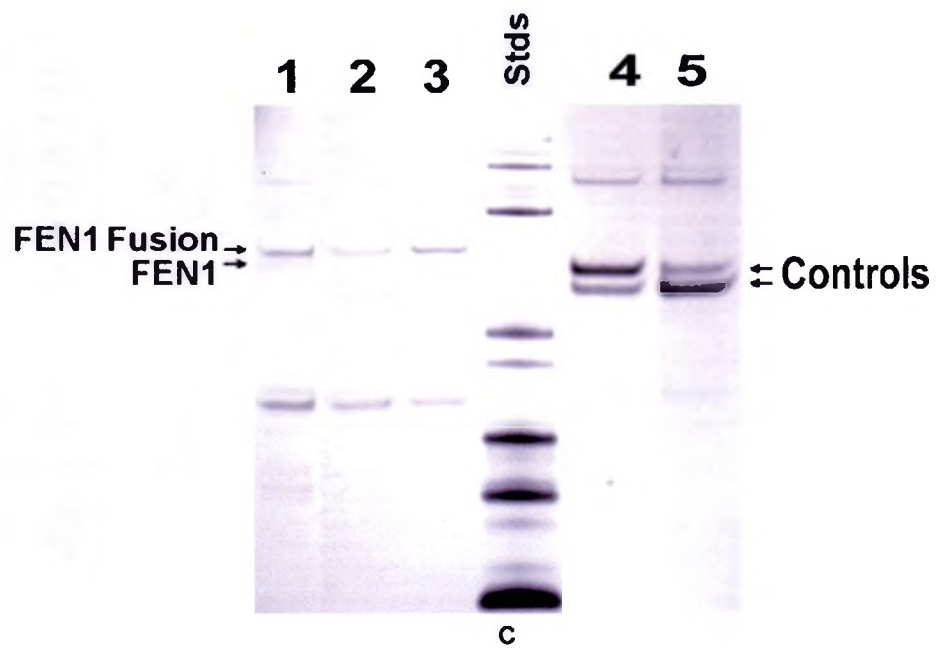
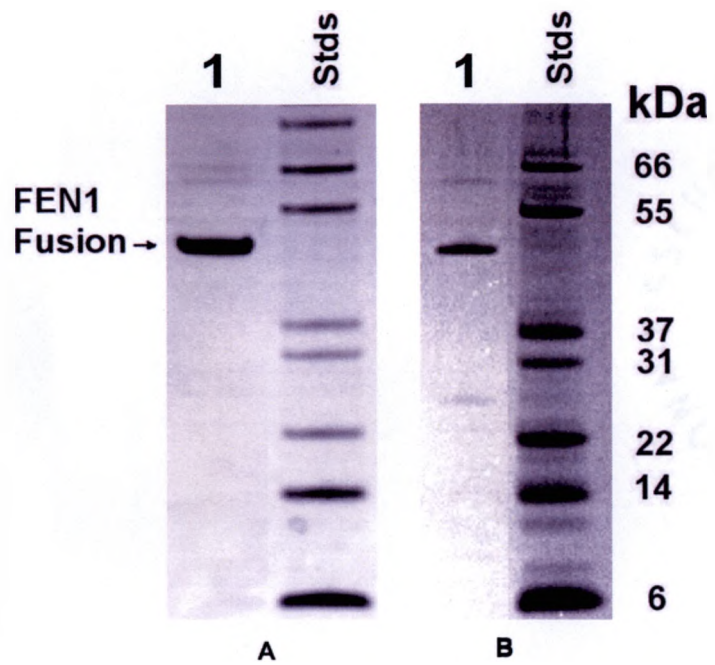


Figure 3-6: MALDI-TOF analysis of xiFEN1ct. Peptide product analysis by MALDI-TOF of PAGE purified xiFEN1ct subjected to in-gel tryptic digestion. Peaks of the resultant mass spectrum that corresponded to tryptic digest predicted fragments are listed in Table 3-2. In addition, several peaks were sequenced by post source decay tandem TOF analyses.

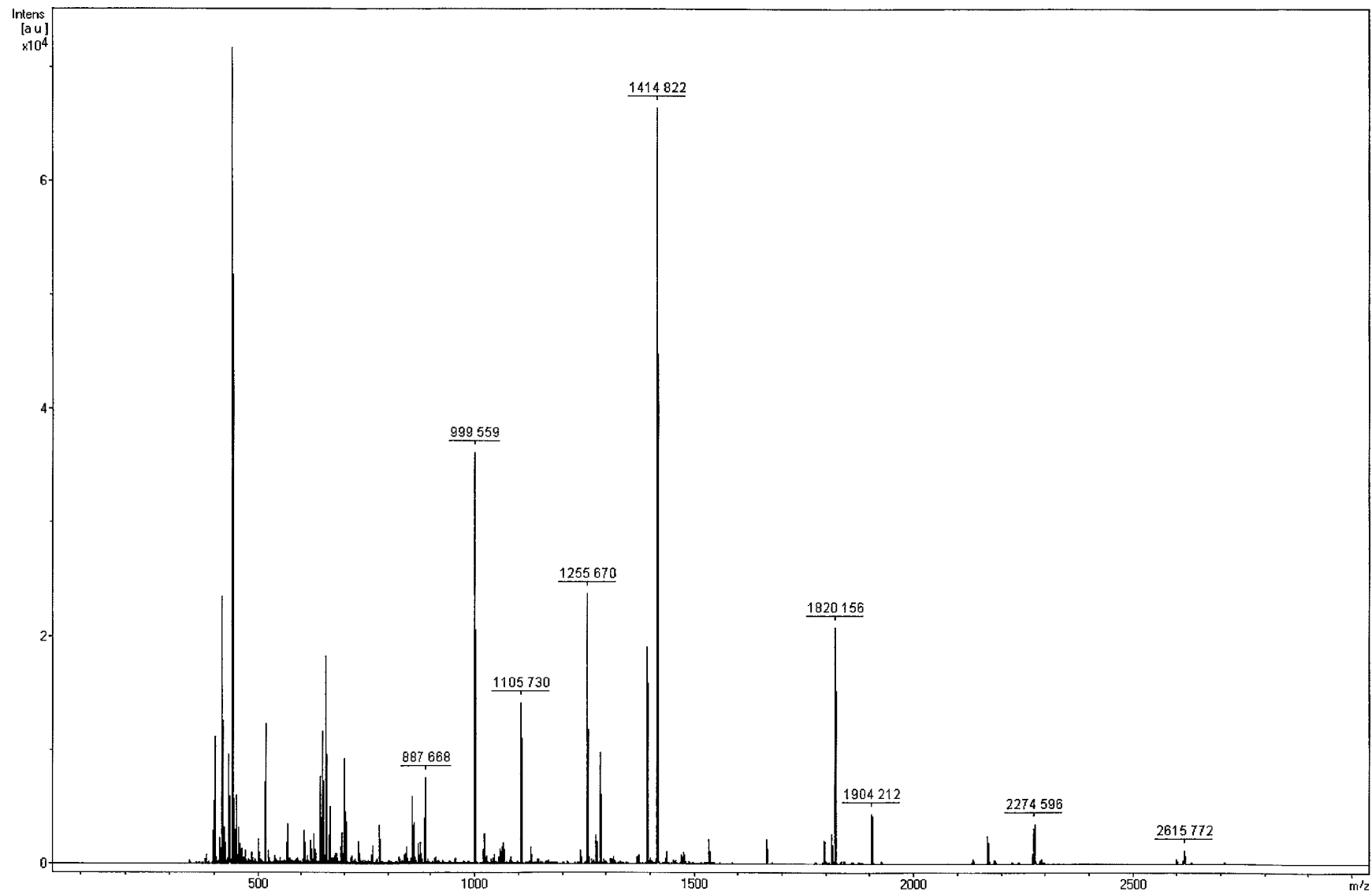


Table 3-2: MALDI-TOF analyses of xiFEN1 tryptic peptides. Spectrum peaks corresponding in mass to predicted (calculated) tryptic digestion fragments of the xiFEN1 fusion proteins are listed. **(A):** XiFEN1ct, MW 46192, 412 residues. **(B):** XiFEN1nt, MW 46778, 416 residues.

A

Spectrum peptide monoisotopic m/z	Calculated monoisotopic m/z	Peptide Mass Fingerprint	Sequence position
826.643	826.460	MGIHGLAK	1-8
877.244	877.562	FSKRLVK	126-132
887.663	887.495	QKTGATPGK	367-375
917.590	917.342	QHND DCK	136-142
999.559	999.441	TGHHHHHH	405-412
1105.73	1105.64	LIADHAPGAIK	9-19
1255.67	1255.61	HPAPEDWLYK	268-277
1414.82	1414.76	KLPVQEFHFNR	201-211
1474.79	1474.74	LDSFFSVTGSLSK	340-353
1813.03	1812.90	QHGSIEEILENIDTSK	252-267
1820.16	1820.03	LEGKPIPPLLGLDSTR	388-404
1842.12	1842.78	EPDEEALIQFMCSEK	300-314
1904.21	1904.04	NLFLKPEVVDSSVLDK	281-297
2168.26	2168.96	WREPDEEALIQFMCSEK	298-314
2271.49	2271.13	VFATATEDMDGLTFGTNVLLR	172-192
2274.60	2273.24	MLENGIKPVYVFDGKPPQLK	74-93
2615.77	2615.15	QDGNVLQSEDGETTSHLMGMFYR	48-70

B

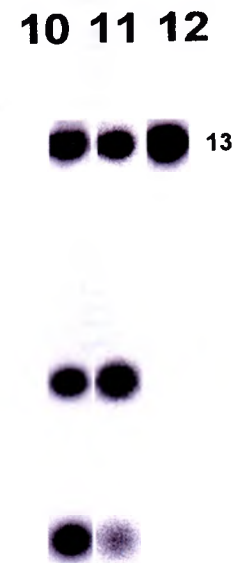
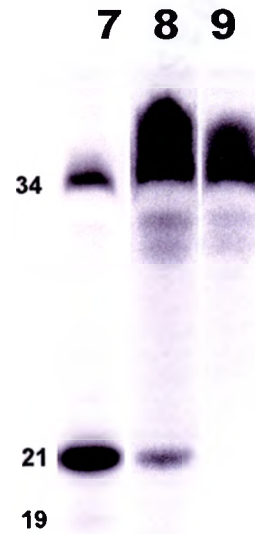
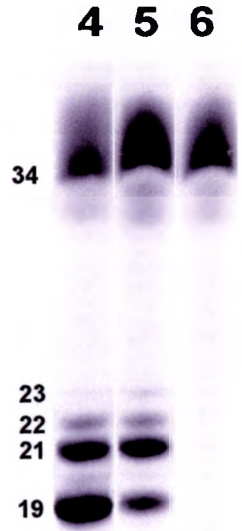
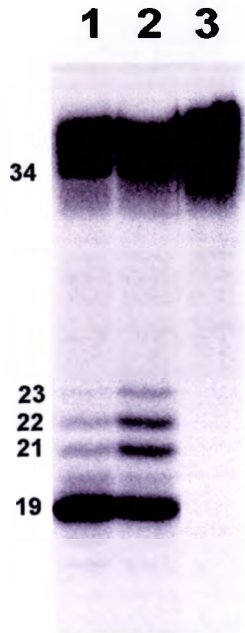
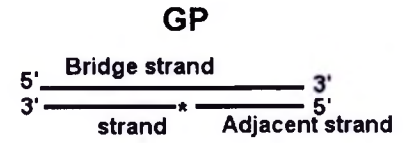
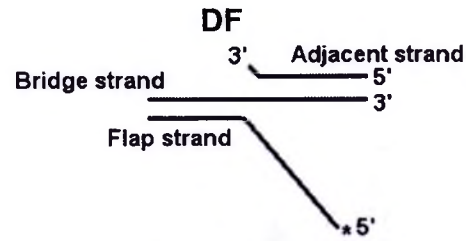
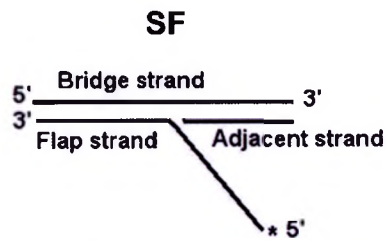
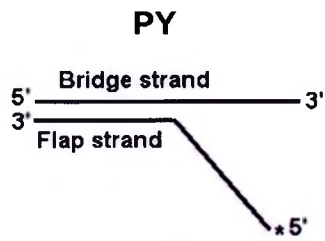
Spectrum peptide monoisotopic m/z	Calculated monoisotopic m/z	Peptide Mass Fingerprint	Sequence position
1255.670	1255.611	HPAPEDWLYK	304-313
1414.920	1414.760	KLPVQEFHFNR	237-247
1904.348	1904.038	NLFLKPEVVDSSVLDK	317-333
2403.642	2403.093	DLYDDDDKDHPFTMGIHGLAK	24-44

XiFEN1 activity and substrate specificity:

Several combinations of oligonucleotides were annealed to assemble known FEN1 substrates (based on expected *in vivo* structures Figure 1-1) in order to assess xiFEN1 enzymatic activity and specificity (3). Five substrates were constructed, four of which are diagrammed in Figure 3-7. As shown, substrates PY, SF and DF consist of a flap structure where the labeled strand comprises the partially unpaired or flap strand (termed the pseudo-Y structure). Substrates SF and DF also possess an annealed strand complementary to the unpaired bridge strand, (termed the adjacent strand, Figure 3-7). This adjacent strand is one nucleotide longer in the DF substrate. It overlaps the point where the flap strand is annealed with the bridge strand creating a double flap structure. The gap substrate (GP) does not contain a flap or pseudo-Y structure and can be derived from substrate SF by complete removal of the unpaired flap plus an additional nucleotide into the double stranded region. This substrate was constructed to test xiFEN1 exonuclease activity. Substrate SS (not shown) consists merely of a single-strand labeled at the 5' terminus.

Ni²⁺IMAC-purified xiFEN1nt did not show activity before or after tag removal. XiFEN1 carboxy-terminal fusion enzyme (xiFEN1ct) exhibited good activity and thus was used along with a commercially acquired recombinant human FEN1 (hFEN1; Trevigen Inc.) for enzymatic characterization and to provide direct comparison of FEN1 activities.

Figure 3-7: xiFEN1 and hFEN1 activities and substrate specificities. Lanes 1, 4, 7 and 10: hFEN1. Lanes 2, 5, 8 and 11: xiFEN1. Lanes 3, 6, 9 and 12: no enzyme. Both enzymes produce multiple products when incubated with the PY and SF substrates. Major product preference differed with xiFEN1 displaying increased cleavage proximal to the flap structure elbow. Band intensities as presented here should only be interpreted qualitatively with respect to other lanes. Images are composites of individual lanes from different experiments.



Neither xiFEN1 nor hFEN1 were able to exhibit measurable levels of activity on substrate SS (data not shown). This is consistent with the known absence of single strand endo- or exonuclease activities for FEN1 enzymes (3).

Both hFEN1 and xiFEN1 enzymes produce mainly a 19-mer cleavage product when incubated with the pseudo-Y structure (Figure 3-7, substrate PY, lanes 1 and 2), however, xiFEN1 produced higher amounts of 21- and 22-mer cleavage products than hFEN1. Data analyses of total versus individual product fractions using substrates PY and SF indicate xiFEN1 and hFEN1 show different activities. Both enzymes produce mainly 19- and 21-mer products when catalyzing the cleavage of substrate SF but xiFEN1 catalyzes more cleavage of this substrate to a 21-mer product, followed by 19-mer; whereas the hFEN1 exhibits the opposite pattern (Figure 3-7, lanes 4 and 5). Overall, the results from substrates PY and SF indicate the fish FEN1 enzyme exhibits a higher preference for cleavage to the longer (i.e., 21-, 22-mer) products rather than the 19-mer product; which is the favored cleavage product for the human FEN1 enzyme. XiFEN1 and hFEN1 both produced a single 21-mer product when incubated with the DF substrate. In addition both produced the same products when digesting the GP substrate illustrating that xiFEN1, like hFEN1 exhibits exonuclease activity on gap structures.

Xiphophorus FEN1 was purified to a specific activity of 2.3×10^5 U/mg compared to the commercially obtained hFEN1 specific activity of 7.8×10^5 U/mg. One unit is defined as the amount of enzyme required to catalyze the

cleavage of one picomole of substrate in one hour at 30°C. These activities were determined using substrate SF with manganese cofactor.

Changes in relative activity with change of substrate and reaction buffer were investigated for each enzyme. Manganese was shown to be the only metal ion cofactor to increase murine FEN1 activity during initial studies of the mammalian form of this enzyme (murine FEN1; 13). We confirmed this to be the case with hFEN1 but not with xiFEN1 revealing some further differences between these two enzymes (see Table 3-3). In general, both enzymes are most active catalyzing substrate DF and least active catalyzing substrate PY, regardless of cofactor. Manganese (versus magnesium cofactor) increases hFEN1 specific activity for substrate PY (~15%) and SF (~35%) while this change in cofactor has the opposite effect on xiFEN1 (Table 3-3). However, both enzymes display an increase in specific activity with manganese cofactor when catalyzing substrate DF cleavage and a decrease in specific activity catalyzing substrate GP. The differences in specific activity of the two enzymes diminishes for most substrates with Mg reaction buffer (Table 3-3).

Change in activity with temperature was also investigated using substrate SF with magnesium cofactor. Both enzymes showed an increase in relative activity with temperature, identical in the lower range (4-20°C, Figure 3-9). Human FEN1 activity may reach a maximum before xiFEN1.

Interestingly, cleavage site preferences also changed with changes in temperature or reaction buffer. Analysis of data acquired with substrate SF indicated that both enzymes favored larger products with an increase in

temperature. Trends of change in cleavage site preference with reaction buffer were also similar for the hFEN1 and xiFEN1 enzymes. Both enzymes produced more of the larger cleavage products in the presence of manganese (Figure 3-10).

Steady state kinetic data were obtained for substrate SF at 30°C by varying the initial substrate concentration from 5 to 2000 nM in various experiments. Sets of data points were fitted to both the Michaelis-Menten equation by non-linear regression and to the Lineweaver-Burke equation by linear regression methods (Graphpad Prism™ software, Figure 3-8B). Values were obtained for both combinations of xiFEN1 and hFEN1 with magnesium or manganese containing reaction buffer and are presented in Table 3-4. Ratios of 19- or 21-mer product to total product (where total product was determined from total DLU of the gel lane versus DLU of the area encompassing substrate remainder) were nearly identical throughout the entire initial substrate concentration range for both enzymes in all cases (Figure 3-10B). Any differences observed were non-reproducible and remained within a standard deviation of less than 4% from the average value obtained. These small differences were therefore considered to be due to experimental error. Initial velocities were derived directly from the fraction of product (versus unreacted substrate), initial substrate concentration and reaction time. Values of relative change in initial velocity with initial substrate concentration are therefore the same for each product that maintains an unchanged ratio to the total product formed throughout the kinetic range. This leads to identical K_m values for such

products. K_m values obtained in these experiments are therefore reported as an average of those obtained for individual products. Unlike K_m , other kinetic parameters such as V_{max} and k_{cat} are different for each product formed even when the relative product fractions remain the same. Substrate specificities reported here (Table 3-4) are calculated from the turnover numbers of total product formed (substrate disappearance).

Overall, both xiFEN1 and hFEN1 enzymes show an increase in K_m with a change from manganese to magnesium containing reaction buffer although this increase is more pronounced with xiFEN1. Since hFEN1 also increases V_{max} and xiFEN1 decreases V_{max} of substrate SF catalysis with this buffer change, the marked difference in catalytic efficiency between the hFEN1 and xiFEN1 enzymes is very much dependent on cofactor and substrate type.

Table 3-3: Variance in specific activity with change in substrate and cofactor. Values were obtained by averaging at least three individual sets of two reactions. In any reaction set, all conditions other than the type of metal ion cofactor were held constant. All reactions were performed at 30°C and activities derived from total product formed (equivalent to the amount of substrate consumed).

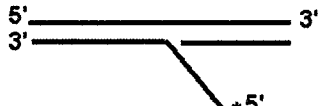
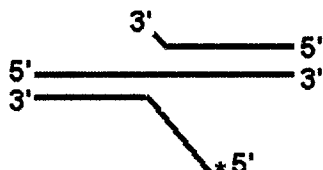
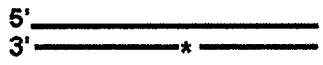
Substrate	hFEN1 (U/ng)		xiFEN1 (U/ng)	
	Mn	Mg	Mn	Mg
PY 	0.12 +/- 0.05	0.10 +/- 0.06	0.0005 +/- 0.0004	0.028 +/- 0.009
SF 	0.78 +/- 0.016	0.52 +/- 0.018	0.23 +/- 0.015	0.56 +/- 0.024
DF 	1.6 +/- 0.33	1.2 +/- 0.25	1.0 +/- 0.28	0.86 +/- 0.19
GP 	0.25 +/- 0.07	0.29 +/- 0.05	0.17 +/- 0.06	0.21 +/- 0.05

Figure 3-8: Determination of steady state kinetic parameters. **(A)** Substrate SF was used ranging in initial concentration from 5-200 nM (lanes 1 through 8) in the hFEN1 experiments and from 50-700 nM in the xiFEN1 experiments (bottom set). All other conditions were identical. **(B)** Results of non-linear regression curve fits using Graphpad™ Prism analysis software.

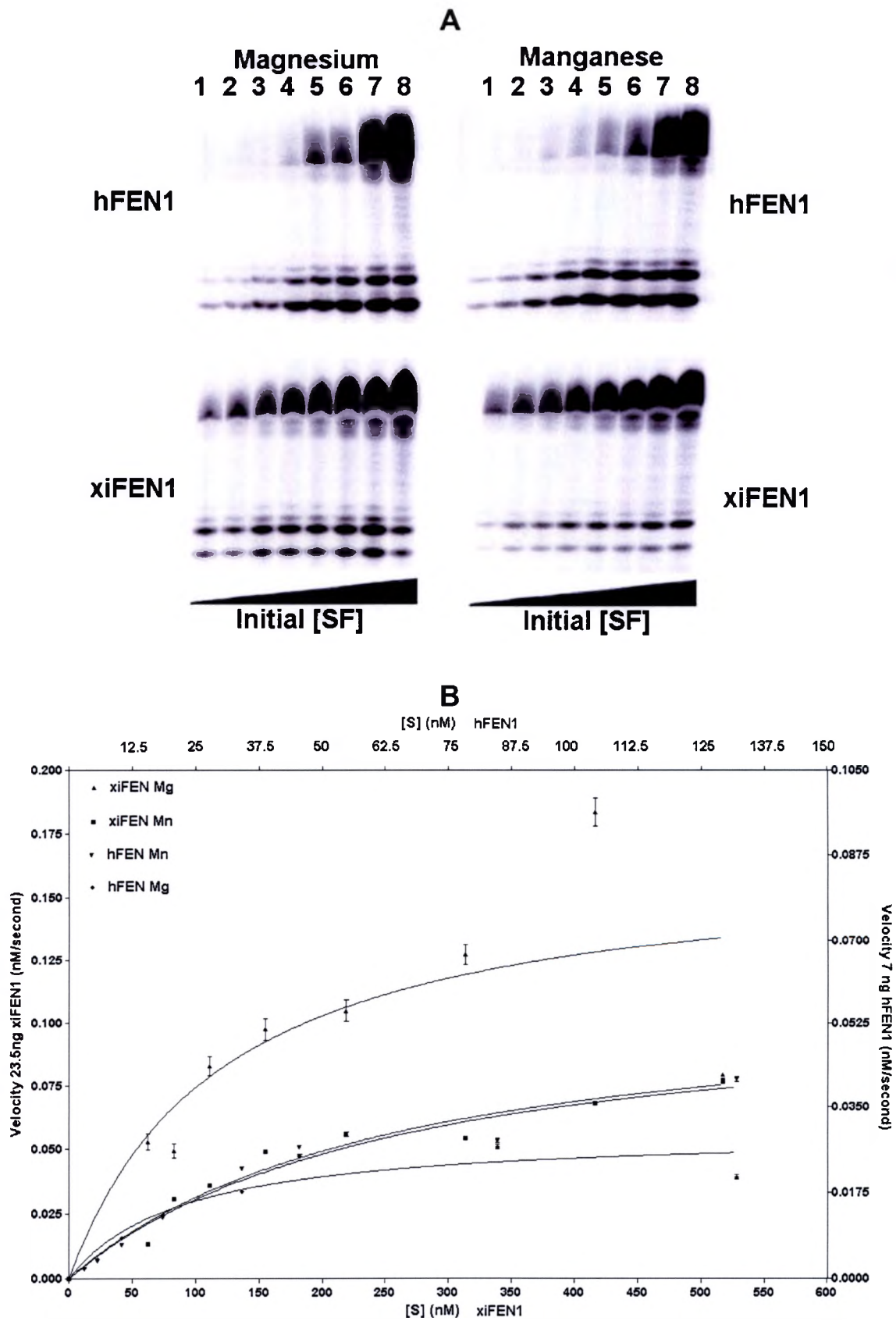


Table 3-4: Michaelis-Menten kinetic data from experiments using single flap substrate and manganese or magnesium cofactor (see Figure 3-7). Values were calculated by fitting data points derived from individual experiments to the Michaelis-Menten equation by non-linear regression (**A**) or to the Lineweaver-Burke equation by linear regression (**B**). Total product formed is directly proportional to the decrease in substrate measured.

		hFEN1	xiFEN1	
A	Mg⁺⁺	K_m (nM)	61	
		k_{cat}/K_m	7.6×10^{-3}	
	Mn⁺⁺	K_m (nM)	79	
		k_{cat}/K_m	1.2×10^{-2}	
	B	Mg⁺⁺	Total	0.46
			19mer	0.28
21mer			0.12	
Mn⁺⁺		Total	0.94	
		19mer	0.46	
		21mer	0.31	
B	Mg⁺⁺	K_m (nM)	91	
		k_{cat}/K_m	1.3×10^{-2}	
	Mn⁺⁺	K_m (nM)	145	
		k_{cat}/K_m	9.1×10^{-3}	
	B	Mg⁺⁺	Total	1.18
			19mer	0.49
21mer			0.29	
Mn⁺⁺		Total	1.32	
		19mer	0.72	
		21mer	0.47	

Figure 3-9: Influence of temperature on enzyme activity. Using substrate SF and magnesium cofactor, temperature was varied from 4°C to 50°C while all other variables were held constant. At each temperature, gel lanes correspond to three dilutions per enzyme and each 7th lane was a no enzyme control as indicated above the image. All values are percentages relative to the highest activity found. XiFEN1 displayed the highest activity at 50°C in all reactions (hence no error bar at this temperature point). Human FEN1 displayed the highest activity at 40°C in two of the three reactions.

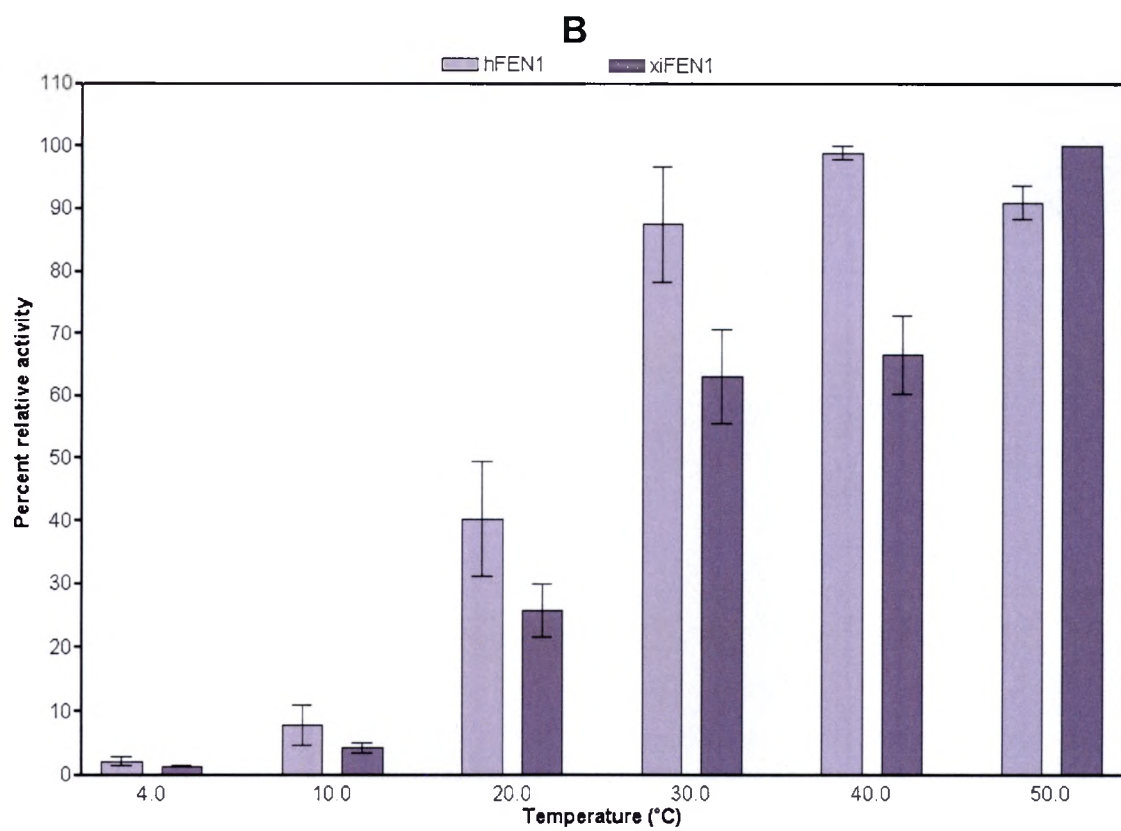
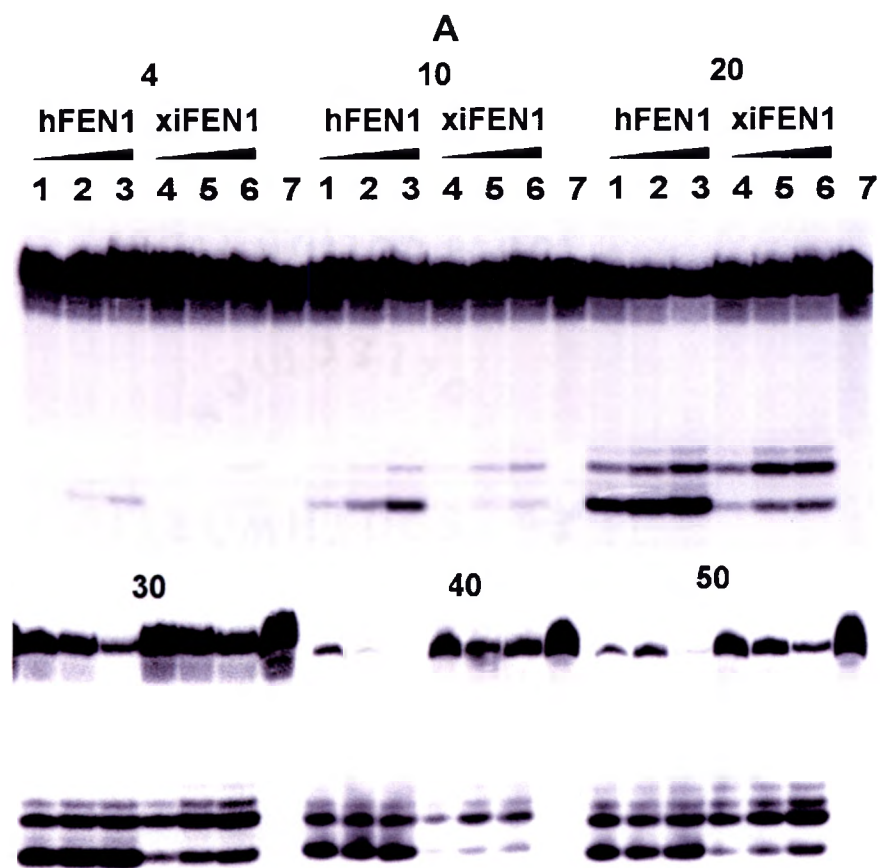
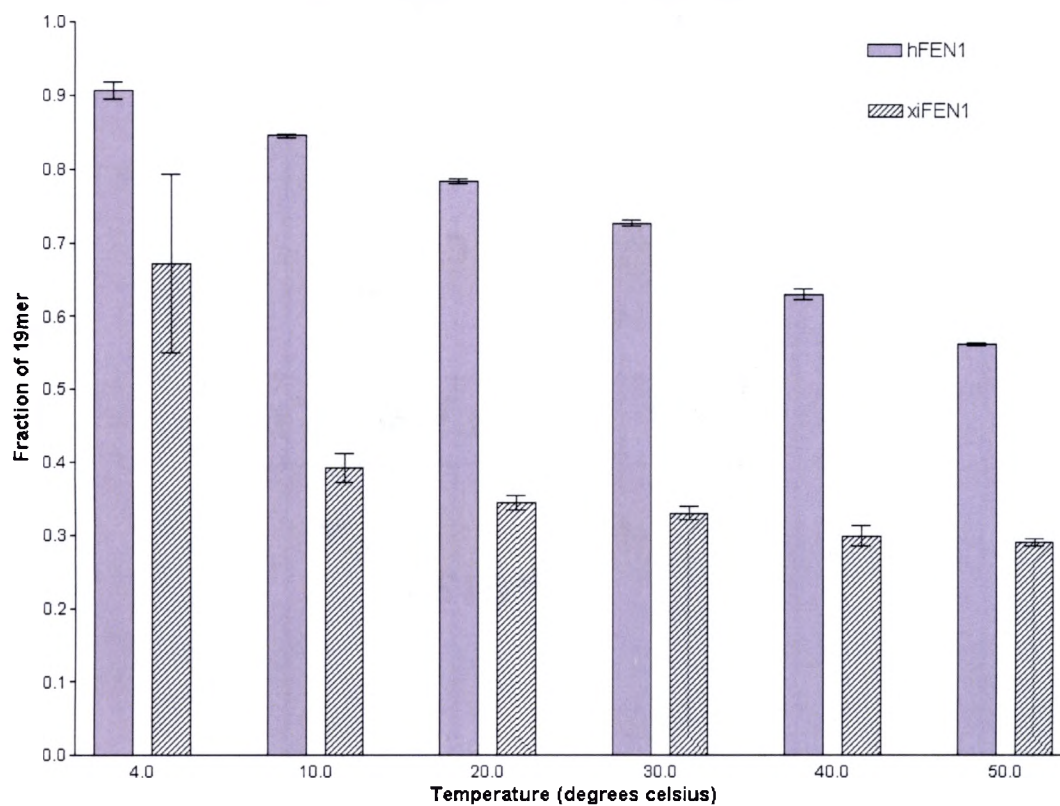


Figure 3-10: Influence of temperature and cofactor on cleavage site preference. **(A)** Influence of temperature cleavage site preference. Data obtained from temperature assays using substrate SF and Mg cofactor. Both enzymes increase the production of larger products with increase in temperature while overall site preference remains opposite. **(B)** Summation of cleavage site preference data obtained from kinetic experiments performed with substrate SF at 30°C. Per enzyme, eight data points were collected at different initial substrate concentrations for each cofactor with all other conditions identical. No change in site preference was observed with change in substrate concentration (see standard deviations) indicating that velocity of individual product formation changes linearly with overall product formation when initial substrate concentration is varied. The same factor of 19- versus 21-mer is produced at each point. However, this factor (cleavage site preference) does change with cofactor and similar trends are observed for both enzymes.

A

Influence of temperature on cleavage site preference
where fraction 19mer + 21mer equals 1.0



B

Influence of cofactor on cleavage site preference.

	Mg	Mn
Enzyme	Fraction 19-mer	Fraction 19-mer
hFEN1	0.38 +/- 0.014	0.33 +/- 0.012
xiFEN1	0.70 +/- 0.009	0.62 +/- 0.009

CHAPTER IV

DISCUSSION

The cloning and high-level expression of flap endonuclease-1 (xiFEN1) from *Xiphophorus maculatus* are presented. In addition, the first reported complete gene structure for a vertebrate FEN1 was deduced and is presented (Figure 3-2). The deduced amino acid sequence derived from the xiFEN1 cDNA open reading frame demonstrates a high degree of similarity and identity with sequences reported for the zebrafish, frog, and human FEN1 forms. The xiFEN1 amino acid sequence was observed to contain many highly conserved basic residues that have been shown to be involved in DNA binding, including R29, R47, R70, R73, R100, R103, R104, K80, K93, and K99 (27). These residues are likely important in establishing and maintaining electrostatic contacts between the FEN1 enzyme and DNA backbone. In addition to these important residues, xiFEN1 also contains the highly conserved acidic residues D34, E160, and D233 which are thought to be involved in coordination of divalent metal cations, such as Mg²⁺ and Mn²⁺, that are required for full enzymatic activity (8, 10). However, although the alignment of FEN1 amino acid sequences from diverse organisms display very high similarities, we have identified several interesting differences between fish and mammalian FEN1 proteins. For example, a pattern of serine-

cysteine differences are observed in the *Xiphophorus* FEN1, including S38C, S157C, and S232C. Each of these serine-to-cysteine differences comparing human versus *Xiphophorus* FEN1 occurs proximal to one of the metal-coordinating residues, D34, E160, or D233 (10). In addition, examination of the frog FEN1 sequence shows that only two of these three cysteine changes are present, with one of the cysteines (C232) replaced with serine, as observed in the mammalian forms (Figure 3-1). Although the significance of these differences is unknown, they may represent important adaptive changes in the enzyme between the fish and mammalian hosts, with frog representing an intermediary position in the evolution of this enzyme.

The cloning and overexpression of the recombinant *Xiphophorus* FEN1 enzyme in an *E. coli* expression system resulted in the purification of a protein exhibiting flap endonuclease and exonuclease activities similar to FEN1 enzymes from other sources (9, 13, 28, 29). Western blot and mass spectrometric analyses of the expressed proteins confirmed expression of the xiFEN1 fusion proteins. The xiFEN1ct protein was enzymatically active while the xiFEN1nt fusion protein was not. Attempts were made to remove the xiFEN1nt N-terminal tag by enterokinase digestion as described in results (Figure 3-5). No enterokinase (EK) activity was observed under standard conditions. Unfolding the protein under partially denaturing conditions revealed some possible enterokinase cleavage but the xiFEN1nt/xiFEN1 fraction recovered still did not show measurable activity. This is consistent with previous efforts to utilize this amino tag purification mechanism (28). An explanation for the xiFEN1nt

resistance to EK digestion and the lack of activity of this N-terminal fusion protein may be the position of the N-terminus in the enzyme active site pocket, possibly obscuring the fusion tag EK recognition site while at the same time disrupting the active site (10).

Further work in this study was done utilizing xiFEN1ct. We assayed the activity of this recombinant enzyme using a variety of substrates and cofactors and found the activities mirror those reported for other FEN1 enzymes, including archaebacterial (9) and murine forms (3, 13). Enzymatic activity as a function of temperature, cofactor, substrate type and initial substrate concentration were determined and compared to hFEN1 in this study.

Both enzymes displayed the same trends in relative activity with substrate change from SF to DF, GP or PY as described (Table 3-3). Trends in relative activity with change in cofactor from magnesium to manganese were similar for both enzymes using substrates DF and GP, showing activation and deactivation respectively, but were opposite when using substrates SF and PY (Table 3-3). With these latter substrates, hFEN1 was enhanced by the change to manganese whereas the xiFEN1 was suppressed. It is uncertain which cofactor is to be expected *in vivo* for FEN1. It is therefore difficult to speculate on the biological necessity for observed changes in enzymatic activity with change in cofactor. However, investigation of such changes may provide us with new insights into the FEN1 structure and reaction mechanism.

Two of the flap substrates used in this study, consisting of pseudo-Y (substrate PY) and single flap (substrate SF) oligonucleotide structures, have

been previously shown to generate multiple cleavage products upon incubation with FEN1 (13). The predominant products resulting from FEN1 cleavage of this substrate are 19- and 21-mer oligonucleotides resulting from cleavage either one nucleotide proximal or distal to the flap structure “elbow” (3, 13). The proximal cleavage site must occur within the double-stranded region of the substrate resulting in removal of the 21-mer flap oligonucleotide and leaving the remaining oligonucleotide structure containing a single nucleotide gap. On the other hand, cleavage of the flap structure at the closest single-strand point, one nucleotide distal to the “elbow” region, results in release of a 19-mer radiolabeled product, and leaves a single-nucleotide flap still in place.

The results presented here utilizing substrate SF show that both the human and *Xiphophorus* FEN1 enzymes catalyzed generation of the expected major products (Figure 3-7). In addition, both enzymes increased production of larger cleavage products with increased temperature (Figure 3-9A) and with change in metal ion cofactor from magnesium to manganese (Figure 3-9B). However, although the same trends with temperature and cofactor were observed, the human and *Xiphophorus* FEN1 enzymes displayed an interesting difference in overall cleavage site preference. The human FEN1 enzyme demonstrated the expected preference for generation of the 19-mer product over the 21-mer product, as is typical for the mammalian enzyme forms (13). On the other hand, the xiFEN1 displayed the opposite behavior, exhibiting generation of the 21-mer product in preference over the 19-mer.

FEN1-catalyzed cleavage of substrate PY also displayed differences in generation of the cleavage products, and hence cleavage site preferences. In general, xiFEN1 displayed increased cleavage preference proximal to the flap structure elbow with the generation of multiple cleavage products (Figure 3-7). Hence, the results indicate the xiFEN1 enzyme exhibits a relatively greater activity than hFEN1 for cleavage at double-stranded substrate sites, producing both 21-mer and larger products.

Although the human and *Xiphophorus* enzymes share highly conserved active site amino acid residues, some marked differences between these enzymes have been demonstrated for several substrates tested. The underlying mechanisms for these observed differences are unknown but we may speculate that one or more of the key amino acid differences described are responsible. A previous study by Qiu et al (27) demonstrated that a site-directed mutant hFEN1 containing an R47A difference shifted the cleavage preference site from position 19 to position 21 for both the pseudo-Y and flap oligonucleotide substrates. In addition, the R47A mutant also displayed a higher K_m (76.3 nM) versus the wild-type enzyme (45.2 nM), thus demonstrating that changes in non-catalytic-site amino acid residues in FEN1 can have a significant effect on both the cleavage site preferences as well as steady-state kinetics.

We observed differences in steady-state kinetics (including K_m) comparing the *Xiphophorus* FEN1 and the human form, even though the *Xiphophorus* R47 residue is conserved. As shown in this study, the xiFEN1 displayed a three-fold greater K_m and ten-fold lower catalytic efficiency (k_{cat}/K_m) than observed for the

hFEN1 (Table 3-4). These differences were measured utilizing substrate SF with manganese cofactor and found to be much less pronounced but still present with reaction buffer containing magnesium cofactor. The large difference in catalytic efficiency for this substrate is in part due to the opposing nature of cofactor change affecting hFEN1 and xiFEN1 k_{cat} values. Catalytic constant values obtained with magnesium cofactor were very similar for hFEN1 and xiFEN1 and overall trends in change of K_m with cofactor were similar for both enzymes; a change to magnesium cofactor appeared to result in a lower K_m for both enzymes (Table 3-4).

As mentioned, we speculate that the marked differences in certain kinetic parameters between the two enzymes may also be due to one or several key amino acid differences near the conserved R47 residue. In particular, both the *Danio* and *Xiphophorus* FEN1 sequences contain D49 residues, instead of a neutral G49 residue found in the human sequence. Considering that the R47 residue may be involved in electrostatic interactions between the enzyme and DNA backbone, the presence of the acidic D49 residue may modify this interaction thus resulting in the observed increase in K_m value for xiFEN1 versus hFEN1. This would be analogous to the K_m increase observed for the R47A mutant reported by Qiu et al. (27).

Enzymatic response to change in temperature was investigated. Both hFEN1 and xiFEN1 demonstrated an increase in activity with temperature in the initial range that may follow a change in reaction rate predicted by the Arrhenius equation. However, human FEN1 showed a level-off or decrease at the highest

temperature assayed and appears to be optimal at about 40°C. XiFEN1 on the other hand was most active at 50°C. In addition the enzymes show a difference at 40°C, possibly due to a change in slope of xiFEN1 activity after 30°C (Figure 3-9).

A change in measured relative enzyme activity in response to a variable other than initial substrate concentration (such as substrate type, cofactor or temperature as discussed above) in a set of experimental conditions could be due to a change in K_m even if the initial set of conditions included saturating substrate concentration. Changes in temperature and cofactor in this case are likely to cause a change in K_m . Since a reduction in activity due to an increase in K_m could be reversed by an increase in substrate concentration, a higher K_m could be interpreted as an indication of the concentration of the substrate in question needed or allowed in that particular biological environment. However, concentrations of 5' flap, recessed, gap or nicked DNA structures that should be maintained in the native environments of human or *Xiphophorus* FEN1 in order to be beneficial for the respective organism is beyond the scope of this study.

Since kinetic data are not available for substrate DF, we do not know whether its activation by manganese (as opposed to magnesium) is due to a change in K_m . The magnesium cofactor could possibly cause this parameter to be increased for this substrate. Figure 3-8 (see corresponding values in Table 3-4) illustrates an example of an increased K_m for the single flap substrate with manganese cofactor for both enzymes while xiFEN k_{cat} is decreased and hFEN k_{cat} is increased. This illustrates that even though only one variable is changed at

the time under these experimental conditions, other parameters may be affected such that useful insight from certain observations may only be gained with complete kinetic analyses. Other factors such as cofactor inhibition and pH dependence have been investigated for FEN1 (13, 27) and these factors may also vary with substrate type and enzyme origin.

Additional study of xiFEN1 may include the effect of site-directed mutagenesis of the D49 to a G49 residue (as found in the human sequence) on the steady-state kinetic and cleavage site preferences for non-mutant versus D49G *Xiphophorus* FEN1 recombinant enzymes. Another interesting set of amino acid differences in human versus *Xiphophorus* (and *Danio*) sequences that may be considered for site directed mutagenesis are the S38C, S157C, and S232C changes found near the conserved metal cation-coordinating residues D34, E160, and D233 respectively. We speculate the presence of the cysteine versus serine residues in the fish FEN1 enzymes may also contribute to differences in steady-state kinetics, metal cation preferences (e.g. Mg²⁺ versus Mn²⁺) and possibly cleavage site preference. In particular, replacement of serine with cysteine residues may alter both the coordination and redox environments near or at the known metal binding sites in the FEN1 structure. Site-directed mutagenesis studies in which the cysteines at positions 38, 157, and 232 are systematically converted to both alanine and serine residues to determine what effect these residues have on metal ion binding, substrate cleavage site specificities, and steady state kinetics of wild-type versus mutant fish FEN1 proteins are currently underway.

LITERATURE CITED

- 1) Waga S, Stillman B. Anatomy of a DNA replication fork revealed by reconstitution of SV40 DNA replication *in vitro* (1994). *Nature*, 369, pp207-212.
- 2) Yoon J, Swiderski PM, Kaplan BE, Takao M, Yasui A, Shen B, Pfeifer GP. Processing of UV Damage *in vitro* by FEN-1 proteins as part of an alternative DNA excision repair pathway (1999). *Biochemistry*, 38, pp4809-4817.
- 3) Harrington JJ, Lieber MR. Functional domains within FEN-1 and RAD2 define a family of structure specific endonucleases: implications for nucleotide excision repair (1994). *Genes Dev.*, 8, pp1344-1355.
- 4) Matsuzaki Y, Adachi N, Koyama H. Vertebrate cells lacking FEN-1 endonuclease are viable but hypersensitive to methylating agents and H₂O₂ (2002). *Nucl. Acids Res.*, 14, pp3273-3277.
- 5) Tishkoff DX, Filosi N, Gaida GM, Kolodner RD. A novel mutation avoidance mechanism dependent on *S. cerevisiae* RAD27 is distinct from DNA mismatch repair (1997). *Cell*, 88, pp253-263.
- 6) Gordenin DA, Kunkel TA, Resnick MA. Repeat expansion - all in a flap? (1997). *Nature Genetics*, 16, pp116-118.

- 7) Liu Y, Bambara RA. Analysis of human flap endonuclease 1 mutants reveals a mechanism to prevent triplet repeat expansion (2003). *J. Biol. Chem.*, 278, pp13728-13739.
- 8) Shen B, Nolan JP, Sklar LA, Park MS. Functional analysis of point mutations in human flap endonuclease-1 active site (1997). *Nucl. Acids Res.*, 25, pp3332-3338.
- 9) Hosfield DJ, Frank G, Weng Y, Tainer JA, Shen B. Newly discovered archaeobacterial flap endonucleases show a structure-specific mechanism for DNA substrate binding and catalysis resembling human flap endonuclease-1 (1998). *J. Biol. Chem.*, 273, pp27154-27161.
- 10) Hwang KY, Baek KW, Kim H, Cho Y. The crystal structure of flap endonuclease-1 from *Methanococcus jannaschii* (1998). *Nat. Struct. Biol.*, 5, pp707-713.
- 11) Kim C, Park MS, Dyer RB. Conformational change upon binding to the flap DNA substrate and location of the Mg²⁺ binding site (2001). *Biochemistry*, 40, pp3208-3214.
- 12) Zheng L, Li M, Shan J, Krishnamoorthi R, Shen B. Distinct roles of two Mg²⁺ binding sites in regulation of murine flap endonuclease-1 activities (2002). *Biochemistry*, 41, pp10323-10331.
- 13) Harrington JJ, Lieber MR. The characterization of a mammalian DNA structure specific endonuclease (1994). *The EMBO Journal*, 13, pp1235-1246.

- 14) Bae KW, Baek KW, Cho CS, Hwang KY, Kim HR, Sung HC, Cho Y. Expression, purification, characterization and crystallization of flap endonuclease-1 from *Methanococcus jannaschii* (1999). *Mol. Cells*, 9, pp45-48.
- 15) Walter RB, Kazianis S. *Xiphophorus* Interspecies Hybrids as Genetic Models of Induced Neoplasia (2001). *ILAR J.*, 42, pp299-322.
- 16) Walter RB, Rains JD, Russell JE, Guerra TM, Daniels C, Johnston DA, Kumar J, Wheeler A, Kelnar K, Khanolkar VA, Williams EL, Hornecker JL, Hollek L, Mamerow MM, Pedroza A, and Kazianis S. A microsatellite genetic linkage map for *Xiphophorus* (2004). *Genetics*, 168, pp363-372.
- 17) Kazianis S, Nairn RS, Walter RB, Johnston DA, Kumar J, Trono D, Della-Coletta L, Gimenez-Conti I, Rains JD, Williams EL, Mamerow MM, Kochan KJ, Scharl M, Vielkind JR, Voff J-N, Woolcock B, Morizot DC. The genetic map of *Xiphophorus* fishes represented by 24 multipoint linkage groups (2004). *Zebrafish*, 1, pp287-304.
- 18) Vielkind JR, Kallman K, Morizot DC. Genetics of melanomas in *Xiphophorus* fishes (1989). *J. Aquat. Anim. Health*, 1, pp69-77.
- 19) Kazianis S, Gimenez-Conti I, Setlow RB, Woodhead AD, Harshbarger JC, Trono D, Ledesma M, Nairn RS. MNU induction of neoplasia in a novel fish model (2001). *Laborat. Invest.*, 81, pp1191-1198.
- 20) Setlow RB, Woodhead AD, Grist E. Animal model for ultraviolet radiation-induced melanoma: platyfish-swordtail hybrid (1989). *Proc. Natl. Acad. Sci. USA*, 86, pp8922-8926.

- 21) Nairn RS, Morizot D, Kazianis S, Woodhead AD, Setlow RB. Nonmammalian models for sunlight induced carcinogenesis: genetic analysis of melanoma formation in *Xiphophorus* hybrid fish (1996). *Photochem. Photobiol.*, 64, pp440-448.
- 22) David WM, Mitchell DL, Walter RB. DNA repair in hybrid fish of the genus *Xiphophorus* (2004). *Comp. Physiol. & Biochem.*, 138, pp301-309.
- 23) Mitchell DL, Meador JA, Byrom M, Walter RB. Resolution of UV-induced DNA damage in *Xiphophorus* fishes (2001). *Mar. Biotechnol.*, 3, pp61-71.
- 24) Mitchell DL, Nairn RS, Johnston DA, Byrom M, Kazianis S, Walter RB. Decreased levels of DNA excision repair in hybrid fish of the genus *Xiphophorus* (2004). *Mut Res. Photochem. Photobiol.*, 79, pp447-452.
- 25) Walter RB, Sung HM, Obermoeller RD, Mitchell DL, Intano GW, Walter CA. Relative base excision repair in *Xiphophorus* fish tissue extracts (2001). *Mar. Biotechnol.*, 3, pp50-60.
- 26) Oehlers LP, Heater SJ, Rains JD, Wells MC, David WD, Walter RB. Gene structure, purification and characterization of DNA polymerase β from *Xiphophorus maculatus* (2004). *Comp. Biochem. Physiol. C*, 138, pp229-409.
- 27) Qiu J, Bimston DN, Partikian A, Shen B. Arginine residues 47 and 70 of human flap endonuclease-1 are involved in DNA substrate interactions and cleavage site determination (2002). *J. Biol. Chem.*, 277, pp24659-24666.
- 28) Bibikova M, Wu W, Chi E, Kim K, Trautman JK, Carroll D. Characterization of FEN-1 from *Xenopus laevis* (1998). *J. Biol. Chem.*, 273, pp34222-34229.

- 29) Kao HI, Henricksen LA, Liu Y, Bambara RA. Cleavage specificity of *Saccharomyces cerevisiae* flap endonuclease-1 suggests a double-flap structure as the cellular substrate (2002). *J. Biol. Chem.*, 277, pp14379-14389.
- 30) Stromo GD. Identifying Coding Sequences. In: *Nucleic Acid and Protein Sequence Analysis: A Practical Approach* (1987). Bishop and Rawlings, eds. pp231-258. IRL Press, Oxford England.

